

Star Formation and Molecular Clouds at High Galactic Latitude

Peregrine M. McGehee

*Infrared Processing and Analysis Center,
California Institute of Technology,
Pasadena, CA 91125 USA*

Abstract. In this chapter we review the young stars and molecular clouds found at high Galactic latitudes ($|b| \geq 30^\circ$). These are mostly associated with two large-scale structures on the sky, the Gould Belt and the Taurus star formation region, and a handful of molecular clouds including MBM 12 and MBM 20 which, as a population, consist of the nearest star formation sites to our Sun. There are also a few young stars that are found in apparent isolation far from any molecular cloud. The high latitude clouds are primarily translucent molecular clouds and diffuse Galactic cirrus with the majority of them seen at high latitude simply due to their proximity to the Sun. The rare exceptions are those, like the Draco and other intermediate or high velocity clouds, found significantly above or below the Galactic plane. We review the processes that result in star formation within these low density and extraplanar environments as well as the mechanisms for production of isolated T Tauri stars. We present and discuss the known high-latitude stellar nurseries and young stellar objects.

1. Introduction

The young stellar populations at high Galactic latitude ($|b| \geq 30^\circ$) are predominately associated with two structures, the Taurus-Auriga star formation region and the Gould Belt, that each subtend large areas on the sky. Pre-main-sequence stars have been verified in a handful of, generally the densest, high-latitude molecular clouds: MBM 12 (Luhman 2001), MBM 20 (L1642; Sandell, Reipurth, & Gahm 1987), and possibly MBM 33 and MBM 37 (Martin & Kun 1996). A few other high-latitude molecular clouds such as the MBM 18/MBM 19 complex (Chaplin, Larson, & Gerakines 2004) are suspected of harboring active star formation.

Magnani et al. (2000) deduce on statistical grounds a Gaussian scale height for the high latitude clouds [HLC] of ~ 100 pc, consistent with that determined for lower latitude dark clouds. As Magnani, Hartmann, & Speck (1996) note, the HLCs have characteristics that set them apart from the dark clouds, namely lower densities and isotopic CO abundances but higher $W(^{12}\text{CO})/W(^{13}\text{CO})$ ratios.

The nature of HLCs, except for those having systemic velocities not consistent with differential Galactic rotation, can be understood in the context of the evolutionary scenario outlined by Stark & Lee (2005). The origins of the intermediate [IVC] and high velocity clouds [HVC], as these exceptions are known, are a matter of significant study.

The initial stage in the formation of molecular clouds is that atomic gas clouds having a velocity dispersion $\sim 12 \text{ km s}^{-1}$ and scale height ~ 100 pc condense from the diffuse atomic gas. As the condensation process continues, the cloud cores become

increasingly molecular resulting in low mass ($< 100M_{\odot}$) high latitude clouds characterized by a scale height of ~ 70 pc. The next stage in the cloud growth is the transition, at masses between 100 and $10^5 M_{\odot}$, to fully molecular clouds that have similar scale heights as the partially molecular high latitude clouds and are capable of star formation. Stark & Lee (2005) found that in their analysis of the Bell Laboratories ^{13}CO Milky Way survey the scale height for small molecular clouds ($M < 2 \times 10^5 M_{\odot}$) is roughly independent of cloud size. For the giant molecular clouds [GMC], however, the scale height decreases with mass, with the largest clouds always found in the Galactic mid-plane. This reduced scale height for the GMCs is attributed to the dissipative process of GMC formation associated with passage of a spiral arm.

In this formation scenario all but the very nearest molecular clouds are viewed in projection against the Galactic plane. The high-latitude clouds are therefore either very close to the Sun or high above the Galactic plane, in both cases they warrant careful study of their ability to undergo star formation. Based on Jeans' mass arguments it is clear that these low density clouds provide for difficult star formation environments via gravitational collapse. It should be noted, however, that dense molecular cores have been detected even in Galactic cirrus, e.g. MCLD 123.5+24.9 (Heithausen, Bertoldi, & Bensch 2002). These nearby clouds are ideal laboratories for study of triggered star formation, for example from supernovae or stellar winds (Elmegreen 1998).

In this chapter we begin with the classification of and surveys for high-latitude molecular clouds. In Sect. 3 we discuss the high-latitude PMS stars and summarize a recent inventory of the SIMBAD database. The individual star formation regions are presented in Sect. 4. Finally, in Sect. 5 we comment on the environment and processes of high-latitude star formation.

2. Molecular Cloud Surveys

2.1. Classification of Molecular Clouds

Molecular clouds are classed, following van Dishoeck & Black (1988), into three categories based primarily on the visual extinction (A_V) along the line of sight through the cloud. Diffuse clouds are identified by $A_V < 1$ magnitude, dark clouds are marked by $A_V > 5$ magnitudes, and translucent clouds are those with intermediate values of A_V . This set of criteria also reflects the changes in astrochemistry (van Dishoeck & Black 1988). While the chemistry in diffuse clouds is largely due to photoprocesses and that in dark clouds is dominated by collisional processes, in the translucent clouds we find the conditions in which carbon is being bound up in the form of CO.

The formation of a molecular cloud requires a column density large enough to shield H_2 and CO from the ambient Galactic ultraviolet flux. Hartmann, Ballesteros-Paredes, & Bergin (2001) explain that this protection from disassociation is a necessary but not sufficient condition for the existence of molecular material. Other factors that influence the rate of formation of molecular gas include the gas density, the dust temperature, and pressure forces. The minimum column density required for shielding is $N_{\text{H}} \sim 1\text{--}2 \times 10^{21} \text{ cm}^{-2}$, corresponding to $A_V \sim 0.5\text{--}1$. While the molecular gas content of diffuse clouds is difficult to detect in emission due to low CO column densities ($\leq 10^{15} \text{ cm}^{-2}$; Magnani, Hartmann, & Speck 1996), optical and UV absorption of CH, CH^+ , CN, CO, and H_2 has been used historically to determine distances and probe physical

conditions of these objects (Williams 1934; Bohlin et al. 1978; van Dishoeck & Black 1989; Penprase et al. 2000). These absorption line studies have been limited to sight-lines of early spectral type (generally O, B, and A) stars due to their nearly featureless spectra.

2.2. Surveys for High-Latitude Clouds

High-latitude clouds are predominately diffuse or translucent and are thus difficult to detect on photographic surveys. The notable exceptions are the Lynds Dark Nebulae identified by Lynds (1962) using Palomar Sky Survey plates covering the sky north of $\delta = -33^\circ$, and extended regions of faint ($SB_V > 25 \text{ mag arcsec}^{-2}$) nebulosity seen in deep imaging surveys. The latter were first identified on the Palomar Sky Survey plates by Lynds (1965a) and in an un-published study (circa 1968) by C. R. Lynds. Sandage (1976) subsequently showed that interpretation of these structures as reflection nebulosities illuminated by the Galactic plane yielded surface brightness predictions deduced from the neutral hydrogen column density that were consistent with observations. Deep *BRI* imaging by Guhathakurta & Tyson (1989) suggest a more complex scenario since although the *B* band surface brightnesses supported the scattered starlight from dust model, the *B - R* and *R - I* colors were generally 0.5-1.0 magnitudes redder than predicted. They interpret this as due to a broad luminescence feature in small hydrogenated carbon grains.

The most effective searches for high-latitude clouds have been based on CO and far infra-red (FIR) dust emission. Early millimeter surveys for molecular clouds using the 115 GHz CO (1-0) transition (Magnani, Blitz, & Mundy 1985; Keto & Myers 1986; Heiles, Reach & Koo 1988) were based on previously identified extinction regions or H I clouds. Magnani, Hartmann, & Speck (1996) provided a compilation based on the literature giving properties and references for clouds with the acronyms UT, ir, HSVMT, G, Stark and 3C. The HRK catalog (Heiles, Reach & Koo 1988) includes clouds in regions studied in H I, CO and the IR. Subsequent blind all-sky CO (1-0) surveys were performed by Hartmann et al. (1998) and Magnani et al. (2000) for the north and south Galactic hemispheres, respectively.

Désert, Bazell & Boulanger (1988) combined IRAS 100 μm data and the Berkeley H I survey (Heiles & Habing 1974) to detect 516 infrared excess clouds (IREC) at $|b| > 5^\circ$. Reach, Wall & Odegard (1998) subsequently created higher-resolution maps based on DIRBE/COBE FIR imaging and the Leiden-Dwingeloo HI survey (Hartmann & Burton 1997) finding 81 new clouds (DIR - Diffuse Infrared Clouds). de Vries, Heithausen & Thaddeus (1987) conducted a search for FIR emission excess indicative of the presence of H_2 in cold clouds within the Ursa Major region.

High latitude clouds identified by FIR excess emission and having $E(B - V) > 0.15$ magnitudes are commonly detected in CO(1-0) (Chastain et al. 2006) but not at lower reddenings, thus FIR and CO surveys are sensitive to different cloud populations. Assuming $R_V = 3.1$, this value of $E(B - V)$ corresponds to $A_V \sim 0.5 \text{ mag}$ which is well below the traditional $A_V \sim 1$ boundary between diffuse and translucent clouds thought to mark the onset of CO formation. The ability of high latitude clouds to more readily form molecular cores is due to the decreased ambient UV interstellar field. In the high latitude environment the UV field is thought to be primarily from extragalactic sources and a factor of 2 or 3 lower than the standard value in the solar neighborhood of $(1 - 2) \times 10^5 \text{ photons cm}^{-2} \text{ s}^{-1} \text{ \AA}^{-1}$ over 1000-2000 \AA . Heithausen, Bertoldi, & Bensch (2002) have detected CO(1-0) emission from molecu-

lar cores in regions having A_V as low as ~ 0.2 magnitudes. As found by Magnani et al. (2003) and Chastain et al. (2006) the correlation between $W(CO)$ and $E(B - V)$ breaks down at low values of $E(B - V)$. Possible mechanisms for this lack of correlation include the increased contribution of dust associated with atomic hydrogen and local variations in grain properties and the radiation field.

The major complexes found in the northern Galactic hemisphere include the Ursa Major cloud complex, which may be physically related to the Polaris Flare as infrared and 21 cm H I observations reveal a common surrounding arc of gas and dust (Meyerdierks, Heithausen, & Reif 1991), the Draco Intermediate Velocity Clouds (MBM 41–44; Goerigk et al. 1983), and the MBM 34 – MBM 37 clouds associated with the L134N dark cloud north of the ρ Ophiuchus star formation region. The southern Galactic sky contains two large structures, the first being the clouds south ($145^\circ \leq l \leq 195^\circ$, $-46^\circ \leq b \leq -30^\circ$) of the Taurus-Auriga star formation region [SFR], the second is the MBM 53-55 complex. The southern Taurus clouds may be unrelated to the Taurus-Auriga SFR due to kinematic considerations (Magnani et al. 2000); however both these clouds and the L134N region are projected near to the Gould Belt.

2.3. Cataloged High Latitude Clouds

In the recent compendium of Galactic dust clouds by Dutra & Bica (2002) only 439 out of 5004 (9%) are found at Galactic latitudes $|b| \geq 30.0$. The Dutra & Bica (2002) catalog is derived from a heterogeneous set of surveys based on IR, CO, and optical detection methods. For the high-latitude clouds the primary sources used, along with their catalog designations and detection techniques, are Magnani, Blitz, & Mundy (1985) [MBM; CO], Keto & Myers (1986) [KM; CO], Désert, Bazell & Boulanger (1988) [IREC; H I and FIR], Magnani, Hartmann, & Speck (1996) [various; literature], and Reach, Wall & Odegard (1998) [DIR, H I and FIR]. Within this high-latitude sample the majority (393, or 90%) have central extinctions less than 1 A_V and are therefore classed as diffuse clouds. In the Dutra & Bica (2002) catalog we find that Lynds 1457, associated with MBM 12, is the sole high-latitude dark cloud, as defined by $A_V > 5$. The remaining 45 clouds (10%) are classed as translucent. The complete set of high-latitude clouds from Lynds (1962) are listed in Table 1 where the A_V extinctions are computed from the “ $E(B - V)_{\text{cen}}$ ” values of Dutra & Bica (2002) assuming $R_V = 3.1$.

The asymmetry between the numbers of northern and southern clouds suggests that these are primarily a local population of objects. In the catalog of Dutra & Bica (2002) we see that 54% of the high latitude diffuse clouds and 63% of the high latitude translucent and dark clouds are found in the Galactic Southern hemisphere. By assuming that the molecular clouds follow a Gaussian distribution with a scale height of 87 pc, Magnani, Hartmann, & Speck (1996) obtain a displacement for the Sun of 14 pc above the mid-plane, consistent with analyses based on star counts, Population I objects, dust, and many other tracers.

3. Pre-Main-Sequence Star Surveys

The search for high-latitude pre-main-sequence stars has a lengthy history primarily based on imaging or objective prism studies. These surveys have targeted the H α and Ca I H&K emission lines (Herbig et al. 1986; Schachter et al. 1996), X-ray emission associated with the magnetospheric accretion process and the magnetic activity of youth, the infrared excess due to circumstellar disk thermal emission, and the nearby stel-

Table 1. Lynds Dark Clouds at $|b| \geq 30^\circ$

Lynds Number	l [deg]	b [deg]	Molecular Cloud	A_V
L134	4.18	+35.75	MBM 36	2.9
L169	5.28	+36.77	MBM 37	1.7
L183, L184	5.70	+36.62	MBM 37	2.1
L1311	125.22	+32.25	IREC 167	1.0
L1312	126.60	+32.18	IREC 167	0.4
L1453	158.66	−33.80	MBM 12	3.8
L1454	158.90	−33.77	MBM 12	4.1
L1457	159.11	−34.45	MBM 12	5.9
L1458	159.14	−33.64	MBM 12	4.2
L1569	189.54	−36.67	MBM 18	1.5
L1642	210.89	−36.51	MBM 20	2.0
L1778	358.97	+36.82	MBM 33	2.0
L1780	359.23	+36.60	MBM 33	1.7

lar associations identified from proper motion studies. Verification of candidate PMS stars requires spectroscopy to confirm the signatures of youth including Li I absorption, Balmer and other emission lines, and low surface gravity.

3.1. $H\alpha$ surveys

Stephenson (1986) surveyed the northern high Galactic latitude sky ($\delta > -25^\circ$ and $|b| > 10^\circ$) searching for candidate $H\alpha$ emission stars using the Burrell Schmidt telescope. A total of 206 candidates were identified on a series of ≈ 1300 5.2×5.2 degree red-sensitive objective prism plates acquired at a dispersion of 1000 \AA/mm and a limiting magnitude ~ 13 . Subsequent spectroscopic follow-ups (Downes & Keyes 1988; Weaver & Hobson 1988; Maheswar, Manoj, & Bhatt 2003; Emprechtinger et al. 2005) of the resultant catalog [StHA] have identified several T Tauri stars including a handful at high Galactic latitude such as StHA 18 in MBM 12.

Kun (1992) conducted a deeper objective prism survey (to $V \sim 16$) with the Schmidt telescope of Konkoly Observatory covering the MBM 23-44, 49, 50, 53, 54 and 55 molecular clouds which resulted in 100 candidate $H\alpha$ emission-line stars. Subsequent spectroscopy at the Isaac Newton Telescope by Martin & Kun (1996) showed that of the 63 best candidates for PMS status, only $\sim 20\%$ were confirmed to have $H\alpha$ in emission and of these only four are T Tauri stars. These four stars, [K92] 35A, 35B, 37, and 54 are found in the L134 complex (MBM 33 and MBM 37).

3.2. IR Surveys

The IRAS mission produced all-sky imaging at 12, 25, 60, and $100 \mu\text{m}$ bands with 10σ sensitivities between 0.65 and 3.0 Jy . The Pico dos Dias Survey (PDS; Gregorio-Hetem et al. 1992; Torres et al. 1995) utilized the IRAS Point Source Catalog (PSC; Joint Science Working Group 1985) to search for young stars including T Tauri stars. Magnani, Caillaut, & Armus (1990) used the PSC to search for low-mass star formation, finding 111 sources projected against 17 translucent and two dark high-latitude ($|b| > 25^\circ$) clouds. A full search covering $|b| > 30^\circ$ using the IRAS Faint Source Survey (FSS; Moshir et al.

1989) was subsequently performed by Magnani et al. (1995) yielding 192 candidates. These surveys targeted objects with the infrared-excess characteristic of thermal emission from circumstellar disks following the work of Beichman et al. (1986) and Myers et al. (1987).

3.3. X-ray Surveys

Optical ($H\alpha$) and IR surveys are sensitive to properties associated with Classical T Tauri stars. Since Weak-lined T Tauri stars do not possess an inner circumstellar disk and thus do not exhibit either the strong emission lines due to accretion or an IR excess due to the disk thermal emission, they are not distinguishable from the field star population. WTTS can, however, be selected in X-ray surveys due to strong emission arising from coronal activity (Feigelson & Decampli 1981).

The Einstein and the ROSAT X-ray satellites were able to detect significant populations of PMS stars. The Einstein Observatory (Giacconi et al. 1979) imaging overlapped 10 of the high-latitude ($|b| > 25^\circ$) molecular clouds in the MBM (Magnani et al. 1995) catalog: MBM 7, 12, 18, 20, 27, 30, 36, 43, 54, and 55. Spectroscopy of the candidate PMS stars in these fields, which are also at $|b| > 30^\circ$, result in only a single confirmed T Tauri star, which is in MBM 12 (Caillault, Magnani, & Fryer 1995). The ROSAT All-Sky Survey (RASS; Trümpler 1983) enabled mapping of the late-type PMS populations around known star formation regions including Taurus and uncovered previously unknown young stars in the Gould Belt and the high-latitude field (Magazzu et al. 1997).

Other X-ray surveys of high-latitude clouds were performed by Hearty et al. (1999) and Hearty et al. (2000b) using ROSAT pointed observations and RASS data. The regions surveyed included the molecular clouds MBM 7, MBM 12, MBM 40, and MBM 53-55. Optical spectroscopy of candidate PMS stars confirmed T Tauri stars in MBM 12 and MBM 55.

3.4. Proper Motion Surveys

A supplementary technique for identification of PMS populations older than 10–70 Myr is the search for clustering in the kinematic and spatial UVWXYZ six-dimensional phase space. When coupled with the ROSAT All-Sky Survey catalog, this has been an effective means of discovering nearby young stellar associations (SACY - the Search for Associations Containing Young Stars Survey; Torres et al. 2006). These local populations are discussed in the chapter by Torres et al. in this Handbook. Application of proper motion and radial velocity surveys over the past several years have resulted in the identification of several nearby stellar groups including TW Hya, β Pic, AB Dor, η Cha, ϵ Cha, Tucana, and Horologium (Zuckerman & Song 2004; López-Santiago et al. 2006).

3.5. OB Stars

Humason & Zwicky (1947) first identified faint blue stars at high Galactic latitudes. These stars can be classified as massive Population I stars ejected from the Galactic disk, as evolved stars such as blue horizontal-branch [BHB] or post-asymptotic giant branch [PAGB] stars, or as young massive stars formed in-situ high above the Galactic disk (Martin 2004). The latter possibility was subsequently ruled out by Martin (2006). The distinguishing features of stars formed in-situ in the halo are that they

should possess halo kinematics and should have abundances consistent with that of the intermediate-velocity [IVC] and high-velocity [HVC] molecular clouds found in this environment.

Wakker (2001) determined the metallicities and abundances for several HVCs and IVCs based on spectra from the FUSE satellite and the STIS and HRS spectrographs on the HST. The derived [Fe/H] values ranged from -1 to 0 (nearly solar) suggesting that these clouds have diverse origins including low-metallicity inflow, possible Galactic fountain clouds, and tidal remnants, for example from the Magellanic Stream.

[Fe/H] values in selected IVCs and HVCs are -0.1 for complex MI, -1.0 for complex CI, -0.6 for the Magellanic Stream, -0.3 for the PP Arch, 0.0 (solar) for IV6, IV9, IV19 and the LLIV Arch. The HVCs appear to be at distances exceeding 5 kpc, while IVCs are generally within 0.5 to 2 kpc. Typical cloud masses are 0.5 to $8 \times 10^5 M_{\odot}$ for IVCs and more than $10^6 M_{\odot}$ for HVCs.

Surveys of high-latitude blue stars, e.g. Martin (2004, 2006), have tended to rule-out in-situ formation in extraplanar environments based on metallicity. As discussed above, near solar metallicities are, however, possible due to injection into the halo of disk material in fountain and superbubble flows. Martin (2006) combined kinematics and abundance information for 49 faint high latitude B stars and found 31 Population I runaways, fifteen old evolved stars (including five BHB stars, three post-HB stars, a pulsating helium dwarf, and six stars of ambiguous classification), one F-dwarf, and two stars that were unclassifiable. Martin (2006) concludes that no star in the sample unambiguously shows the characteristics of a young massive star formed in situ in the halo.

3.6. SIMBAD Database Search

The SIMBAD Astronomical Database was searched for Herbig-Haro Objects [HH] and the following classes of stars: confirmed or candidate Young Stellar Objects [Y*O, Y*?], confirmed or candidate optically detected Pre-Main Sequence Stars [pr*, pr?], confirmed or candidate T Tauri stars [TT*, TT?], Variable Stars of the Orion Type [Or*], and Variable Stars of the FU Ori Type [FU*] over the entire sky. The resulting list of 9621 objects included 932 having positions reported as “No Coord.” which were subsequently removed from consideration. The breakdown of SIMBAD object codes in this discarded set were 886 HH, 7 pr*, 25 TT*, 10 Y*?, and 4 Y*O. 107 of the remaining 8689 objects are found at $|b| \geq 30^{\circ}$.

Seven objects found in the SIMBAD database were discarded from this list due to spurious positions or identifications that resulted in their inclusion in the sample of high-latitude HH objects and young stars. The positions of Herbig-Haro objects HH 458, in Serpens, and HH 26D, in Orion, are incorrectly given in SIMBAD although they are both correct in the literature, see Davis et al. (1999) and Davis et al. (1997), respectively. Two additional HH objects, HH 20G and HH 23G, discovered by Gyul’Budagyan, Glushkov, & Denisyuk (1978) during their inspection of Palomar Sky Survey plates covering $|b| < 10^{\circ}$, had spurious positions reported by SIMBAD. The massive YSOs [MCB2004b] G41.9 A1 and [MCB2004b] G41.9 A2 (Mercer et al. 2004) discovered by the Spitzer Galactic Legacy Infrared Mid-Plane Survey Extraordinaire (GLIMPSE) Legacy Program are also given incorrect positions by SIMBAD. Finally, although [DG97] 2-1 has an Optical ID of “YSO faint” in Table 1 of Danziger & Gilmozzi (1997) the text clearly describes this X-ray source as a candidate AGN.

Table 2. SIMBAD Query Results for Young Stars

Object Type	Code	All-Sky	$ b \geq 30^\circ$	Galactic
Herbig-Haro Object	HH	2071	6	2
Young Stellar Object	Y*O	2809	13	1
PMS Star (optically detected)	pr*	641	30	2
T Tauri Star	TT*	1188	58	55
Variable Star of the Orion Type	Or*	729	0	0
Variable Star of the FU Ori Type	FU*	21	0	0
Candidate Young Stellar Object	Y*?	38	0	0
Candidate PMS Star	pr?	842	0	0
Candidate T Tauri Star	TT?	3	0	0
Multiple classifications	Y*O,pr*, TT*,Or*	332	0	0
Star plus Herbig-Haro Object	HH and Y*O,TT*	15	0	0

The results for each class over the entire sky and at high latitudes are summarized in Table 2. The final column of Table 2 gives the number of each class whose positions and identifications have been verified and are Galactic, i.e. not associated with the Large or Small Magellanic Clouds. For completeness we include six objects classed as young stars in Hearty et al. (1999) or in SIMBAD that were subsequently reclassified. These are Hen 3-1 (aka PDS 1; RS CVn: K giant plus G dwarf binary), CD-65 150 (aka PDS 3; a Li-rich K giant), HD 21051 (a K giant, see Smith & Shetrone (2000)), V1129 Tau, a G0 eclipsing binary (Otero et al. 2005), and GSC 04704-00892 and GSC 05282-02210, both ~ 100 Myr old K dwarfs south of Taurus. Hen 3-1 was the basis for the search that resulted in the discovery of the ~ 30 Myr old Tucana-Horologium association even though it was subsequently understood to not be a member (Torres et al. 2000). GSC 04704-00892 and GSC 05282-02210 are examples of X-ray active stars with weak Li I absorption that are part of the general young, but not PMS, population.

The results from SIMBAD were supplemented by 10 stars listed in Hearty et al. (1999) that had SIMBAD classifications not indicative of a PMS status. Of these, 3 are classed as components of a Spectroscopic Binary [SB*], 2 as Emission-Line Stars [Em*], 2 as Variable Stars [V*], 2 as Stars [*], and 1 as a Peculiar Star [Pe*]. In Table 3 we list the complete set in order of increasing Galactic latitude with the exception of the six reclassified stars which are grouped together at the end. Each table contains the star name (from SIMBAD), the Galactic coordinates, the spectral type, and parent molecular cloud or present-day association. We include the half-dozen $H\alpha$ emission-line stars projected against MBM 18 that Hearty et al. (1999) attribute to an unpublished paper by Brand et al. The assignment of molecular cloud or association was based on the referenced literature. The distinction between the Taurus-Auriga and South Taurus populations generally falls along lines of Galactic longitude with the former having $l < 174$, the one exception being the star TYC 664-764-1 identified by Li & Hu (1998).

Table 3.: Young stars at $|b| \geq 30^\circ$

Star	l [deg]	b [deg]	SpT	Object Type	Cloud or Association	Notes
HD 141569	4.18	+36.92	B9.5e	pr*	...	1
[K92] 54	4.26	+36.74	M5.5IV	Em*	MBM 37	2,3
V* BP Psc	78.58	-57.22	mid-F	TT*	...	4,30
2MASS J23101857+1447203	89.51	-41.43	M3V	TT*	MBM 55	14
[LH98] 1	155.00	-35.89	G8V	TT*	Tau-Aur	5
[FS2003] 0101	156.28	-32.50	M:	TT*	Tau-Aur	5,6
[LH98] 19	156.52	-32.53	K4V	TT*	Tau-Aur	5
V* AP Ari	156.66	-30.51	K0	TT*	Tau-Aur	5
[LH98] 3	157.69	-38.03	F7V	TT*	Tau-Aur	5
GSC 01230-01002	158.65	-34.05	K6	TT*	MBM 12	7
HD 18831	158.74	-31.24	F5	TT*	Tau-Aur	5
EM* LkHA 262	158.83	-33.98	M1IIIe	TT*	MBM 12	7,8
EM* LkHA 263	158.83	-33.98	M3	Em*	MBM 12	7,8,9
[HNS2000] 42	158.84	-33.92	M5.7...	TT*	MBM 12	7,10
[L2001] 8	158.86	-33.31	M5.5	TT*	MBM 12	7
V* WY Ari	158.92	-33.89	K3:...	TT*	MBM 12	7,8
1E 0255.3+2018	159.01	-33.34	K3msp	TT*	MBM 12	4,7
[L2001] 10	159.02	-33.28	M3.2...	TT*	MBM 12	7
[L2001] 9	159.27	-33.64	M5.7...	TT*	MBM 12	7
[HNS2000] 53	159.38	-34.07	M3	Y*O	MBM 12	9,10
[L2001] 6	159.51	-33.92	M5	TT*	MBM 12	9,10
[L2001] 11	159.70	-33.95	M5.5	TT*	MBM 12	9
TYC 646- 530-1	159.96	-39.95	G4V	TT*	Tau-Aur	5
BD+21 418	160.64	-30.03	G5	TT*	Subgroup B4	29
[G82b] 3	161.38	-35.93	...	HH	MBM 13	11

Continued on next page

Table 3 – continued from previous page

Star	l [deg]	b [deg]	SpT	Object Type	Cloud or Association	Notes
[LH98] 20	161.57	−38.16	G0V	TT*	Tau-Aur	5
EM* StHA 18	162.31	−35.50	M3	TT*	MBM 12	7,10
HD 17662	163.35	−41.47	G5	TT*	Tau-Aur	5
[LH98] 53	163.97	−31.67	...	TT*	Tau-Aur	12
TYC 1240- 336-1	163.97	−31.67	G0V	TT*	Tau-Aur	5
HD 18580	164.00	−38.40	K2	TT*	Tau-Aur	5
[LH98] 40	164.79	−37.19	G5IV	TT*	Tau-Aur	5
TYC 644- 257-1	165.18	−40.31	K0	TT*	Tau-Aur	5
GSC 00644-00256	166.31	−41.74	...	TT*	Tau-Aur	5
[LH98] 35	166.53	−40.23	K7	TT*	Tau-Aur	5
TAP 3	166.99	−33.91	...	TT*	Tau-Aur	13
TYC 655- 1494-1	169.67	−36.32	G2IV	TT*	Tau-Aur	5
RX J0314.7+1127	169.72	−38.06	M1V	TT*	Tau-Aur	14
RX J0326.3+1131	172.29	−36.11	M2V	TT*	Tau-Aur	14
RX J0328.0+1114	172.89	−36.02	M3V	TT*	Tau-Aur	14
[LH98] 79	174.55	−33.12	K0V	TT*	South Tau	5,16
GSC 00653-00192	174.56	−35.59	K3	TT*	South Tau	17
TYC 664- 764-1	175.93	−30.84	G7IV	TT*	Tau-Aur	5
GSC 00060-00489	180.24	−42.71	K4	pr*	South Tau	17
GSC 00659-00051	180.50	−31.76	K3	TT*	South Tau	17
GSC 00067-01152	180.75	−40.19	K7	TT*	South Tau	17
RXJ0344.9+0359	183.11	−37.86	K2	*	South Tau	17,18
RXJ0354.4+0535	183.41	−35.02	G2	*	South Tau	17,18
~6 stars	189.11	−36.02	...	H α Em	MBM 18	Brand et al. [unpub]
[ATZ98] A123	189.30	−35.14	M4V	TT*	South Tau	18
HD 25457	190.74	−36.87	F5V	TT*	AB Dor	14,18,19
GJ 3305	198.63	−30.66	M0.5	TT*	β Pic	20,21

Continued on next page

Table 3 – continued from previous page

Star	l [deg]	b [deg]	SpT	Object Type	Cloud or Association	Notes
GSC 04744-01367	203.15	−30.00	...	TT*	...	22
HH 123	210.82	−36.61	...	HH	MBM 20	23
HBC 410	210.82	−36.61	...	Pe*	MBM 20	8,24
V* EW Eri	210.86	−36.56	K7IV	V*	MBM 20	8,24
BD-15 808	211.86	−37.51	G4V	TT*	MBM 20	14
HD98800Aa	278.40	+33.80	K5V	SB*	TW Hydrae	22
HD98800Ba	278.40	+33.80	K7V	SB*	TW Hydrae	22
HD98800Bb	278.40	+33.80	M1V	SB*	TW Hydrae	22
TYC 8474-24-1	293.77	−64.10	F2	TT*	...	22,27
2MASS J14104963-2355290	325.33	+35.47	K2	TT*	Gould Belt	28
HD 125340	327.80	+35.22	G6IV	TT*	Gould Belt	28
TYC 6138-383-1	329.46	+42.17	G9	TT*	Gould Belt	28
[K92] 35a	357.84	+37.52	M4V	TT*	MBM 33	2,3
[K92] 35b	357.84	+37.52	M5IV	TT*	MBM 33	2,3
[K92] 37	358.29	+37.78	M4.5IV	TT*	MBM 33	2,3
Reclassified PMS candidates						
HD 21051	170.87	−35.66	K0III-IV	TT*	Tau-Aur	5,14,15 [K giant]
GSC 04704-00892	176.98	−56.76	K4	TT*	South Tau	17 [~100 Myr ZAMS]
V* V1129 Tau	177.40	−32.32	G0	TT*	South Tau	5 [Eclipsing binary]
GSC 05282-02210	178.40	−63.33	K0	TT*	South Tau	17 [~100 Myr ZAMS]
Hen 3-1	280.58	−59.07	dKe?	V*	Horologium	22,25 [RS CVn]
CD-65 150	283.37	−46.19	K1III	TT*	...	22,26 [Li-rich K giant]
Continued on next page						

Table 3 – continued from previous page

Star	l [deg]	b [deg]	SpT	Object Type	Cloud or Association	Notes
Notes: 1. Weinberger et al. (2000); 2. Kun (1992); 3. Martin & Kun (1996); 4. Magnani et al. (1995); 5. Li & Hu (1998); 6. Fuhrmeister & Schmitt (2003); 7. Luhman (2001); 8. Magnani, Caillaud, & Armus (1990); 9. Luhman & Steeghs (2004); 10. Hearty et al. (2000a); 11. Gyul’Budagyan (1982); 12. Li (2004); 13. Feigelson et al. (1987); 14. Li, Hu, & Chen (2000); 15. Smith & Shetrone (2000); 16. Neuhäuser et al. (1997); 17. Neuhäuser et al. (1995); 18. Appenzeller et al. (1998); 19. Zuckerman, Song & Bessell (2004); 20. Feigelson et al. (2006); 21. Zuckerman et al. (2001); 22. Gregorio-Hetem et al. (1992); 23. Reipurth & Heathcote (1990); 24. Reipurth & Zinnecker (1993); 25. Torres et al. (2000); 26. Gregorio-Hetem, Castilho, & Barbuy (1993); 27. Vieira et al. (2003); 28. Wichmann et al. (1997); 29. López-Santiago et al. (2006); 30. Zuckerman et al. (2008)						



Figure 1. High-latitude star formation regions and young stars in the Northern First and Second Galactic Quadrants ($0^\circ < l < 180^\circ$; $b > 0^\circ$). This region contains the HD 141569 system (**I**) consisting of a Herbig AeBe star and two M stars. The molecular clouds shown are MBM 37 (**H**) and MBM 41-44 (**I**). Within the Polaris Flare are two high-latitude translucent clouds IREC 165 (**N**) and L1311 (**O**). The background is from the dust map of Schlegel et al. (1998).

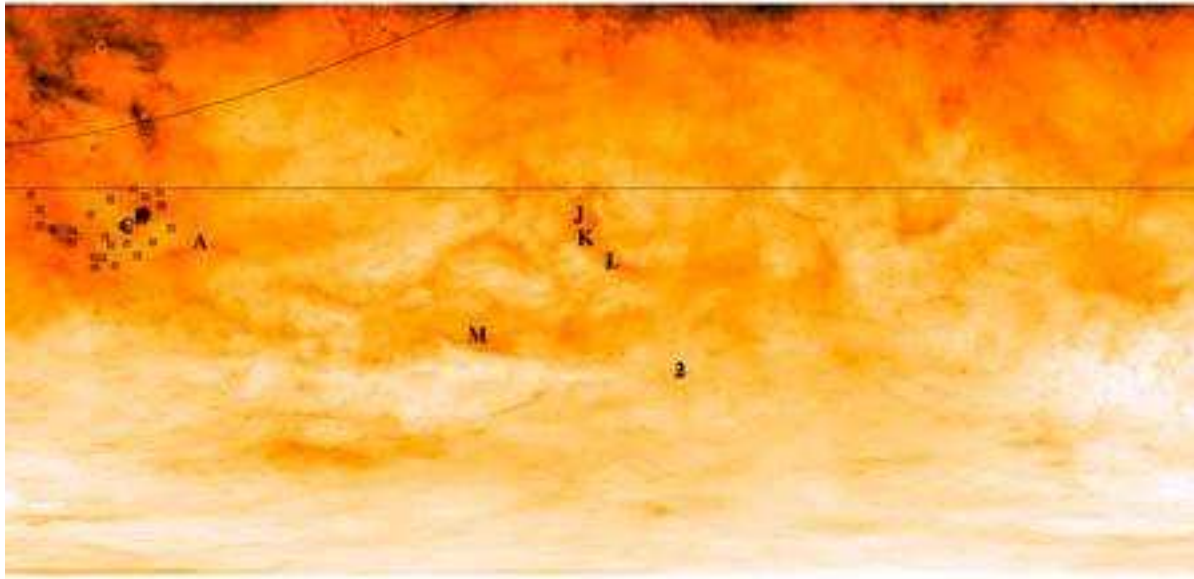


Figure 2. High-latitude star formation regions and young stars in the Southern First and Second Galactic Quadrants ($0^\circ < l < 180^\circ$; $b < 0^\circ$). A second isolated Herbig AeBe star, BP Psc (2), is found in this region. Six molecular clouds - MBM 7 (A), MBM 12 (B), MBM 13 (C), MBM 53 (J), MBM 54 (K) and MBM 55 (L) are identified here. MBM 12 is one of two active high-latitude star formation regions. The southernmost cloud is the translucent cloud IREC 146 (M) which is part of a high-latitude CO shell identified by Chastain et al. (2006). The PMS stars within the South Taurus region are evident in the left-hand portion of this map. The background is from the dust map of Schlegel et al. (1998).



Figure 3. High-latitude star formation regions and young stars in the Northern Third and Fourth Galactic Quadrants ($180^\circ < l < 360^\circ$; $b > 0^\circ$). With the exception of MBM 33 (**G**), a few Gould Belt members, and HD 98800 (TWA 4), this appears to be relatively devoid of recent star formation. The background is from the dust map of Schlegel et al. (1998).

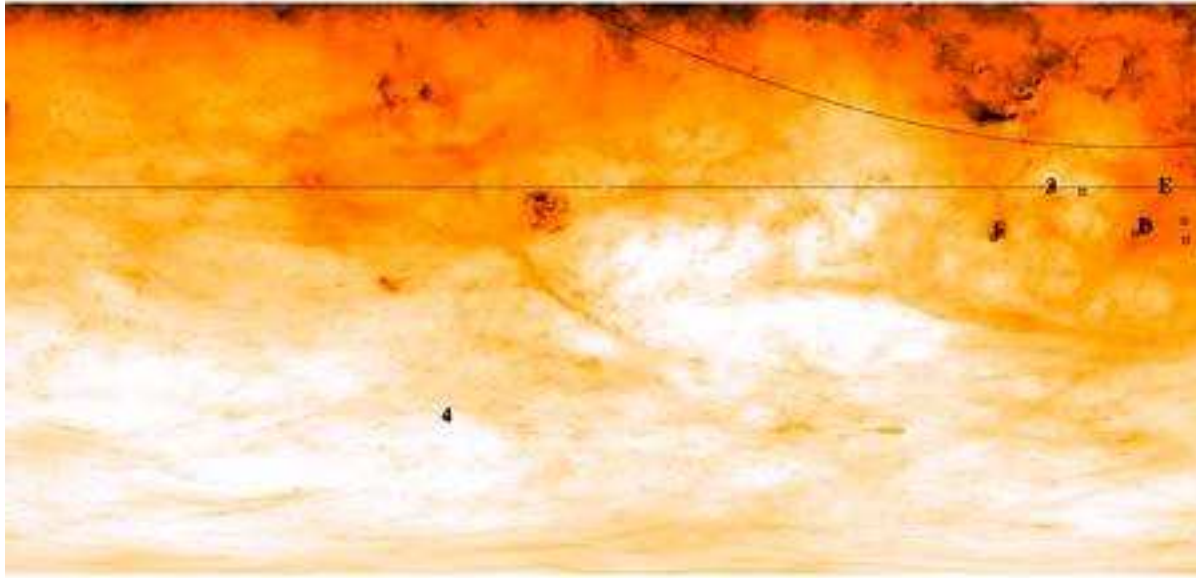


Figure 4. High-latitude star formation regions and young stars in the Southern Third and Fourth Galactic Quadrants ($180^\circ < l < 360^\circ$; $b < 0^\circ$). The isolated PMS stars in this region are GSC 04744-01367 (**3**) and TYC 8474-24-1 (**4**), of which the latter is a Herbig AeBe star. The molecular clouds seen just south of the Taurus and Orion star formation regions are MBM 18 (**D**), MBM 19 (**E**), and MBM 20 (**F**). MBM 18 and MBM 20 contain the Lynds dark clouds L1569 and L1642. L1642 is one of the Orion outlying clouds and is an active star formation region. The background is from the dust map of Schlegel et al. (1998).

4. The High-latitude Star Formation Regions

Pre-main-sequence stars at high Galactic latitude are found as dispersed populations in large-scale structures, within individual molecular clouds, stellar associations, and in isolation. For each region we discuss the distance, age, massive and low-mass stellar populations, and the atomic and molecular gas. Figures 1 through 4 identify the specific molecular clouds and young stars using the Schlegel et al. (1998) extinction maps as backdrops. The background for each image is the Schlegel et al. (1998) FIR-derived dust map displayed on a log scale ranging from $E(B - V) = 0.01$ to $E(B - V) = 3.23$ ($A_V = 10$). Molecular clouds discussed in the text and the three translucent clouds distant from the Gould Belt are marked by letters. The four isolated high-latitude PMS stars are labeled by numbers. The Gould Belt mid-plane and the $|b| = 30^\circ$ definition for Galactic high-latitude are shown for reference.

4.1. Large-scale Structures

The Gould Belt: Gould (1879) noted that the brightest stars on the sky were aligned along a great circle crossing the Milky Way at an angle close to 20° . This structure, known as the Gould Belt, has been the subject of extensive studies over the intervening century.

The Gould Belt appears on the sky as a band approximately 20° wide having an ascending node $l_\Omega = 282^\circ$ and an inclination $i = 24^\circ$, thus the Gould Belt populations appear at $b > 30^\circ$ and $b < -30^\circ$ around $l = 12^\circ$ and $l = 192^\circ$, respectively. The Gould Belt is described as an ellipsoidal shaped ring with semi-major and semi-minor axes of 500 pc and 340 pc (Guillout et al. 1998). The center of this structure is approximately 200 pc distant from the Sun towards $l = 130^\circ$. The composition of the Gould Belt includes interstellar matter and a combination of Population I disk stars of ages up to 80 Myr, OB associations, and young clusters. Proposed formation scenarios for the Gould Belt include collisions of high velocity clouds with the Galactic disk (Comeron & Torra 1992, 1994) or induced star formation from winds originating in supernovae or the central Cas-Tau association (Blaauw 1991). Hartmann, Ballesteros-Paredes, & Bergin (2001) suggest that the Gould Belt is not truly a coherent structure but is due to the motion of interstellar material around and out of the Galactic plane driven by complex and interacting flows.

Wichmann et al. (1997) identified three high-latitude Gould Belt stars near $l = 327^\circ$ in their spectroscopic survey spanning $b = -5^\circ$ to 50° of RASS selected T Tauri candidates in Lupus. Li-rich RASS sources in other regions of the sky, including South Taurus, may be also associated with the Gould Belt.

The Taurus-Auriga Complex: The southern high-latitude skies between $l = 150^\circ$ and $l = 200^\circ$ are dominated by the dispersed stellar populations associated with the young (< 10 Myr) and nearby (140 pc) Taurus-Auriga star formation region (see the chapter by Kenyon et al. in this Handbook). The older Gould Belt populations in this region are 300 to 500 pc distant.

Spectroscopy of optical counterparts of RASS sources south of Taurus by Magazzú et al. (1997) and Martin & Magazzú (1999) shows that a significant fraction of the RASS-selected stars are not young WTTS (Neuhäuser et al. 1995) but, on the basis of their Li abundance, are older post T Tauri stars [PTTS]. The presence of PTTS in the central regions of Taurus suggests that low levels of ongoing star formation have been occurring

there for over 10 Myr. The semi-regular pulsating G0 star V1129 Tau was identified as a possible older member of Taurus-Auriga by Li & Hu (1998) on the basis of significant but weak Li I absorption. V1229 Tau is also classed as an eclipsing binary by Otero et al. (2005).

Variability studies comparing TTS in South Taurus, Taurus-Auriga, and MBM 12 indicate no significant difference in the distribution of rotational periods (Broeg et al. 2006). Given the limited sample sizes this study was unable to distinguish between the ejection and small cloudlet formation scenarios for the dispersed young stars. If disk braking plays a major role in the angular momentum evolution of young stars, then due to the truncation of the circumstellar disk by tidal forces the dispersed population should be rotating more rapidly. Broeg et al. (2006) find periods of 4.7 and 1.34 days for two South Taurus TTS GSC 00653-00192 and GSC 00060-00489, respectively. RXJ0344.9+0359 is clearly variable but no period could be determined. The rotational periods of [LH98] 20 and [LH98] 53 have been found to be 1.0 and 0.7 days (Xing et al. 2007a,b).

4.2. Molecular Clouds

In this section we discuss the individual high latitude clouds that either contain spectroscopically confirmed pre-main-sequence stars or have been suspected of harboring star formation. We use the MBM catalog designations based on the CO (J=1-0) survey of Magnani, Blitz, & Mundy (1985) and the literature review of Magnani, Hartmann, & Speck (1996).

MBM 7: Hearty et al. (1999) conducted spectroscopic followup of ROSAT All-Sky Survey targets projected against MBM 7 ($l = 150.47, b = -38.07$). In their survey of X-ray active stars towards MBM 7 and MBM 55 (see below) Hearty et al. (1999) conclude that the majority, which are both Li-weak and near to the main sequence, are of the general nearby stellar population younger than 150 Myr. The estimated distance to MBM 7 is 75 to 175 pc. This cloud is southwest of the Taurus-Auriga complex and within a large arc of dust and gas that has been swept up by either supernovae or stellar winds. MBM 7 is of interest as a laboratory for triggered star formation processes.

MBM 12/MBM 13: The MBM 12 cloud ($l = 159.35, b = -34.32$) is an active region of low mass formation. MBM 12 includes L1457 which is the only dark cloud as defined by $A_V > 5$ found at high Galactic latitudes. Hearty et al. (2000b) obtain a distance estimate of $58 \pm 5 < d < 90 \pm 12$ based on the presence and absence of Na I D line absorption in stars with Hipparcos parallaxes, which led to the assertion that MBM 12 was the nearest molecular cloud and located well within the Local Bubble of hot ionized gas. Recent studies by Luhman (2001) and Andersson et al. (2002) now suggest that the cloud is at 275 pc. Luhman (2001) found extinction at 65, 140, and 275 pc along the line of sight with the 275 pc distance giving the most plausible location on the H-R diagram. A subsequent analysis by Andersson et al. (2002) find a supporting result of 360 ± 30 pc with a foreground, less opaque, layer of extinction at ~ 80 pc. Straizys et al. (2002) derived a distance estimate of 325 pc based on photometry conducted in the Vilnius seven-color system for 152 stars. T Tauri candidates in MBM 12 have been selected by H α and X-ray surveys, with spectroscopic followup revealing a population of a dozen low-mass PMS stars (Stephenson 1986; Herbig & Bell 1988; Hearty et al. 2000b; Luhman 2001). The latter survey is complete to $0.03 M_\odot$ ($H \sim 15$) with the

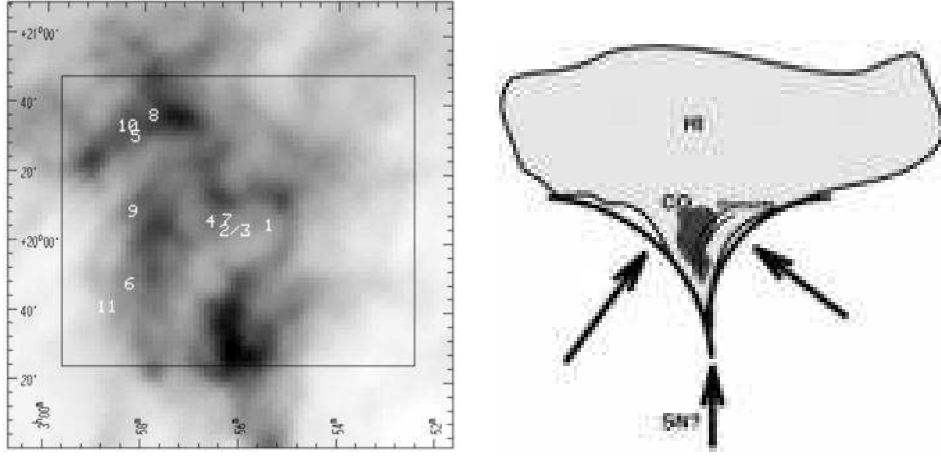


Figure 5. The left panel shows the locations of MBM 12A 1–11 marked on an IRAS 100 μm image of the MBM 12 cloud (from Luhman 2001). On the right (from Moriarty-Schieven, Andersson, & Wannier 1997) is a depiction of a possible triggered star formation scenario due to an external supernova.

verified members having masses down to $0.1 M_{\odot}$. The age of the MBM 12 association is estimated as 2^{+3}_{-1} Myr on the basis of relative Li I strengths and on H-R diagrams (Luhman 2001).

Figure 5 depicts the IRAS 100 μm image of the MBM 12 cloud with the positions of the young stars (MBM 12A 1–12). MBM 12A 2 and 3 (LkH α 262 and 263) are a wide binary system. MBM 12A 12 (StHA 18) is projected against the MBM 13 molecular cloud, 2.5° southeast of MBM 12. MBM 12A 12 is a likely member of this association.

Chauvin et al. (2002) obtained adaptive optics observations with the Canada-France-Hawaii Telescope discovering six binaries, LkH α 264, E 0255+2018, RX J0255.4+2005, StHA 18, MBM 12A 10, RX J0255.3+1915, and confirming the binary nature of HD 17332 (see Figure 6). In addition they detected a possible quadruple system composed of the close binary LkH α 263AB (separation of $\sim 0.41''$), LkH α 262 located $\sim 15.3''$ from LkH α 263A, and of LkH α 263C, located $\sim 4.1''$ from LkH α 263A. The latter is a nebulous object interpreted as a disk oriented almost perfectly edge-on and seen in scattered light. These results suggest that the binary fraction in MBM 12 is high compared to the field and to IC 348.

Broeg et al. (2006) report periodic variability in four MBM 12 TTS attributed to rotational modulation of photospheric features. The inferred rotational period ranged from 3.36 to 7.4 days, although for the CTTS LkH α 264 the observed period differed from results obtained during previous epochs suggesting a more complex mechanism for variability. The WTTS 1E 0225.3+2018 showed strong variability, but poor sampling in this study rendered determination of an accurate period impossible. Pinzón et al. (2006) find the computed mass accretion rates based on *U*-band veiling for GSC 01230-01002 (RXJ0255.4+2005), LkH α 264, and 1E 02553+2018 to be in the range 10^{-8} to $10^{-7} M_{\odot} \text{ yr}^{-1}$, consistent with results from other star formation regions of similar age.

Millimeter continuum observations of TTS in MBM 12 reveal that the disk masses are less than $0.1 M_{\odot}$. These mass limits are consistent with results in Taurus-Auriga

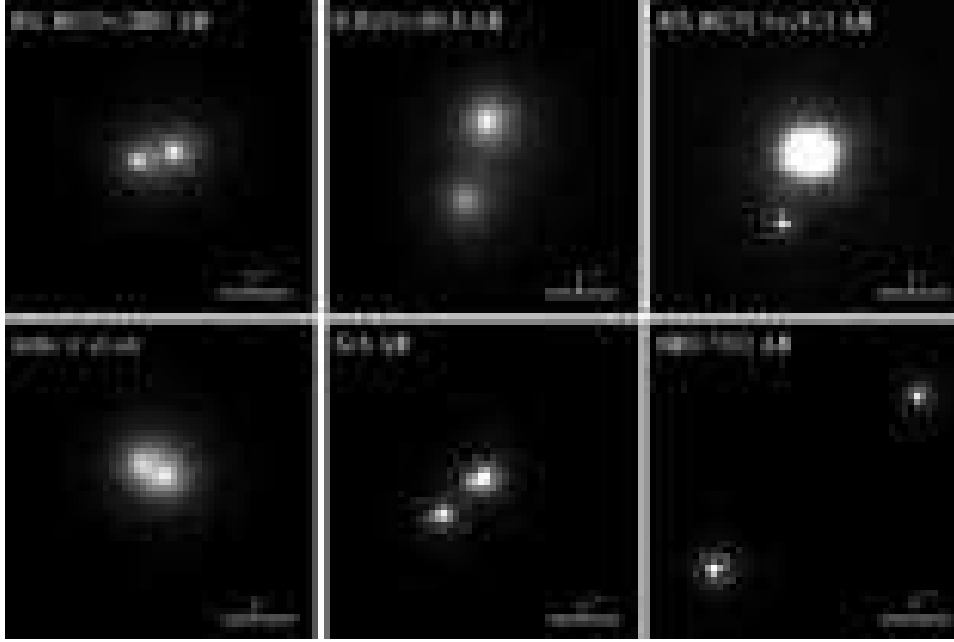


Figure 6. CFHT AO images of binaries in MBM 12 acquired by Chauvin et al. (2002).

and ρ Oph, however massive disks as found around T Tau, DG Tau, and GG Tau can be ruled out. The 3 mm dust continuum survey by Hogerheijde et al. (2002) around eight TTS in MBM 12 (6 in 5 fields; 2 from literature) limits $M_{disk} < 0.04\text{--}0.09 M_{\odot}$ assuming a gas-to-dust ratio of 100 and a distance of 275 pc. Coadding of fields places upper limits on the average disk mass to $0.03 M_{\odot}$. A subsequent survey by Itoh et al. (2003) detected, at the 3σ level and above, emission at 2.1 mm from three MBM 12 TTS. The derived disk masses are $0.048 M_{\odot}$ for LkH α 262, $0.085 M_{\odot}$ for LkH α 264, and $0.071 M_{\odot}$ StHA 18. Based on $450 \mu\text{m}$ and $850 \mu\text{m}$ studies, Hogerheijde et al. (2003) assign dust opacity model dependent masses ranging between 0.02 to $0.2 M_{\odot}$ for LkH α 262 and LkH α 264A. For LkH α 263ABC and StHA 18 Hogerheijde et al. (2003) estimate masses that are an order of magnitude lower.

Honda et al. (2006) find that in a study of 30 TTS, the silicate dust around WY Ari (LkH α 264) has anomalously low large component and crystallinity fractions given the strength of the $10 \mu\text{m}$ silicate feature. The dominant component, as inferred from model fits to N -band spectra, appears to be submicron olivine grains. Honda et al. (2006) speculate that accretion-induced turbulence may allow the smaller grains to drift higher thus making the disk surface rich in small grains.

In their millimeter wave survey [$^{12}\text{CO}(1-0)$, $^{13}\text{CO}(1-0)$, and $\text{CS}(2-1)$] of high-latitude clouds for proto-brown dwarfs, Pound & Blitz (1993) found no clearly self-gravitating low mass clumps in MBM 26, MBM 27–29, MBM 30, MBM 31–32, and MBM 41–44. They did, however, identify two objects in MBM 12 whose masses were within a factor of 3 of being gravitationally bound. One of these two clumps, MBM 12-1, has a dense core detected in $\text{CS}(2-1)$ emission and is apparently in hydrostatic equilibrium.

MBM 16: MBM 16 ($l = 170.60, b = -37.27$) is a large translucent cloud located $\sim 20^\circ$ south of the Taurus clouds. On the basis of interstellar absorption, Hobbs et al. (1988) assigned a distance of 60 to 85 pc. Magnani et al. (2003) adopt a distance of 100 pc, citing arguments concerning X-ray shadowing that MBM 16 is within the boundary of the Local Bubble (Kuntz, Snowden, & Verter 1997; Cox & Reynolds 1987). Four of the WTTS candidates identified by Li, Hu, & Chen (2000) are projected against MBM 16.

MBM 18/MBM 19: The MBM 18 ($l = 189.10, b = -36.02$) and MBM 19 ($l = 186.03, b = -29.93$) clouds have been studied by Brand & Wouterloot (unpublished, see Hearty et al. 1999) who identified candidate T Tauri stars on the basis of $H\alpha$ emission and by Larson and collaborators (Larson & Reed 2003; Chaplin, Larson, & Gerakines 2004). MBM 19 extends north from the MBM 18 high-latitude cloud towards the Taurus SFR and is a suspected site of low-mass star formation. Although MBM 19 exhibits low, relatively smooth $100\ \mu\text{m}$ emission and modest A_V , the $^{12}\text{CO}(1-0)$ in MBM 19 shows clumpy emission with line intensities $> 3\text{K}$. Chaplin, Larson, & Gerakines (2004) find ~ 20 stars within MBM 18 and MBM 19 with possible circumstellar disk signatures on the basis of 2MASS colors. Chaplin, Larson, & Gerakines (2004) determine a distance to MBM 18 (the Lynds dark cloud L1569) of 80 ± 20 pc based on line-of-sight interstellar reddening. They also see only slight evidence for an increase of R_V with increasing A_V suggesting that dust grain growth has not occurred in the denser regions of the molecular cloud.

MBM 20: MBM 20 ($l = 210.89, b = -36.51$) is a member of the Orion outlying clouds discussed in the chapter by Alcalá, Covino, and Leccia in this Handbook. The distance to MBM 20 has been measured as between 100 to 160 pc; significantly closer than the Orion OB1 association (330 to 450 pc). Hearty et al. (2000b) obtain a distance estimate for MBM 20 of $112 \pm 15 < d < 151 \pm 21$ on the basis of Na I D line absorption studies of Hipparcos stars. Lehtinen et al. (2007), based on ISO $200\ \mu\text{m}$ mapping of the L1642 Lynds dark cloud in MBM 20, find evidence for a two-fold increase in the dust emissivity over the temperature range 19 K to 14 K. They attribute this to an increase of the dust absorption cross-section, perhaps due to coagulation of dust grains within the cold molecular core.

Two binary CTTS, L1642-1 (aka HBC 413 and EW Eri) and L1642-2 (aka HBC 410), were identified by Sandell, Reipurth, & Gahm (1987). Evidence for a bipolar outflow is detected in $^{12}\text{CO}(1-0)$ observations near L1642-2 (Liljeström, Matilla, & Friberg 1989). The X-ray active G4V star BD-15 808 identified by Li, Hu, & Chen (2000) is projected within ~ 1 degree of MBM 20. Carpenter et al. (2005) assign an age of 30 to 100 Myr to BD-15 808 and cite a distance of 140 pc, consistent with that of MBM 20. This star was observed during the Formation and Evolution of Planetary Systems (FEPS) *Spitzer* Legacy program and is likely an evolved system based on the lack of an IR excess in the IRAC bands (Silverstone et al. 2006) and little or no emission at 1.2 mm (Carpenter et al. 2005). BD-15 808 may be a member of a general < 150 Myr population noted by Hearty et al. (1999) and not be associated with MBM 20.

MBM 33/MBM 37: MBM 33 ($l = 359.06, b = +36.75$) and MBM 37 ($l = 5.70, b = +36.22$) are cometary globules within the L134 complex located at the northernmost extension of the Sco-Oph star formation region. Early studies of MBM 33 included spectroscopy and multi-band photoelectric observations of the L1778 dark cloud by

Lynds (1965a). Franco (1989) derived a distance of 110 ± 10 pc on the basis of color excess observed in SAO stars of clouds within the region $l = 359^\circ$ to 12° and $b = 35^\circ$ to 39° which includes the dark clouds L134, L169, and L1780. Furthermore, Franco (1989) suggests that these clouds are immersed in a sheet-like absorbing structure related to the surface of the Loop I Bubble.

Two candidate WTTS (K35AB and K37) are identified in projection against MBM 33 (Martin & Kun 1996). These stars have a mid-M spectral type, $H\alpha$ EW of -4 to -9\AA , and Li I EW of 600 to 700 mÅ. An additional WTTS, K54, is seen near MBM 37 having a mid to late M spectral type, $H\alpha$ EW of -15\AA , and Li I EW of 800 mÅ.

Ridderstad et al. (2006) find that the L1780 cloud within MBM 33 contains a dense core having a temperature between 14 K and 15 K, assuming a dust emissivity index $\beta = 2$ and based on IRAS and ISO observations spanning $12\text{ }\mu\text{m}$ to $200\text{ }\mu\text{m}$. There appear to be separate cold and warm dust components as the spatial distribution of the $12\text{ }\mu\text{m}$, $25\text{ }\mu\text{m}$, and $60\text{ }\mu\text{m}$ emission differs from the longer wavelength data that trace the core. The ^{13}CO core of L1780 appears to be in virial equilibrium, but starless, as no candidate young stars are seen in IRAS, ISO, and 2MASS imaging data.

L183 (=L134N), a quiescent cloud lacking signs of protostellar-driven outflow activity, has been a popular subject for astrochemists starting with the H_2CO study by Evans & Kutner (1976). The L134N designation, first used by Evans & Kutner (1976), arises from Lynds (1962) grouping L134, L169, and L183 as different sections of a single object (ID=85). Unlike the dark cloud L1448, which contains the extremely young outflow L1448-mm, L183 is deficit in SiO and complex organic molecules (COMs) such as CH_3OH . Requena-Torres et al. (2007) propose that the observed COM abundances are consistent with a “universal” grain mantle composition that is locally changed by the process of low-mass star formation.

Spectroscopic studies targeting molecular gas phases become difficult in cold cores due to the depletion of molecules onto ice mantles. N_2H^+ and N_2D^+ observations of L183 by Pagani et al. (2007) indicate that the gas is thermalized with the ~ 7 K dust and that N_2H^+ is significantly depleted starting at densities $5\text{--}7 \times 10^5\text{ cm}^{-3}$. Pagani et al. (2007) suggest that the relatively less depleted N_2D^+ is a viable tool for study of cold cores. Akyilmaz et al. (2007) studied the spatial variation of NO abundance in L183 and L1544, another pre-protostellar core, finding evidence for depletion towards the density peaks of each. In the case of L183 the central minimum in the fractional abundance of NO is shifted by 10 arcsec in R.A., or 1000 AU, relative to the dust peak.

L183 is associated with MBM 37 and contains five extinction peaks shown in Figure 7 that related to known molecular peaks. Of these, two are judged by Pagani et al. (2004) to be candidate prestellar cores, of which peak 1 is thought to be more highly evolved due to its logotropic profile (McLaughlin & Pudritz 1997). The total mass of the core at Peak 1 within a radius of 1 arcmin was determined by Pagani et al. (2004) to be $\sim 2.5\text{ M}_\odot$. L183 is designated as a “bright” core by Kirk et al. (2005) who measured integrated flux densities within a 2.5-arcmin diameter aperture of 12.8 Jy at $450\text{ }\mu\text{m}$ and 4.7 Jy $850\text{ }\mu\text{m}$ determining a total mass of 1.8 M_\odot . L183 exhibits different morphologies at these two submillimeter bands with only the denser southern core (Peak 1) being detected at $850\text{ }\mu\text{m}$.

MBM 41–44: The MBM 41–44 complex, also known as the Draco Nebula, is an intensely studied intermediate velocity cloud $v_{lsr} = -21\text{ km/s}$. This object was discovered on the basis of a H I survey conducted by Goerigk et al. (1983). A detailed H I map of the Spitzer First Look Survey by the 100 m Green Bank Telescope (Lockman & Condon

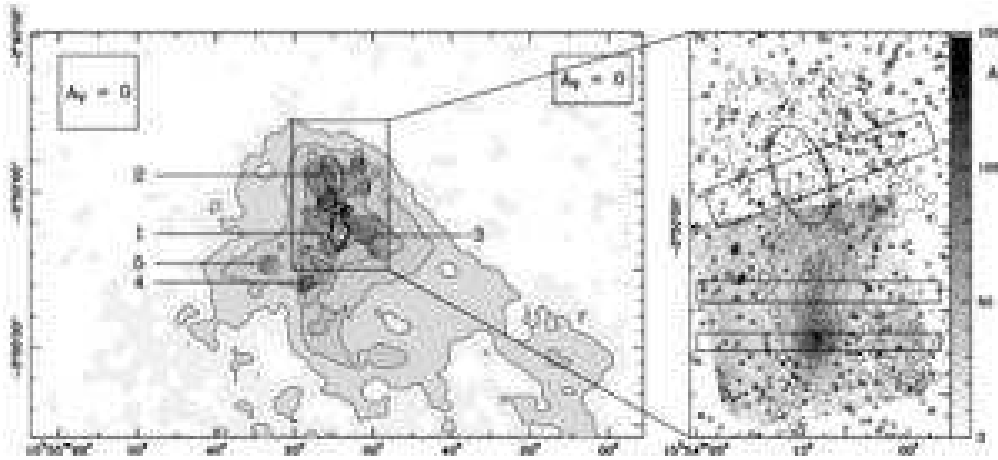


Figure 7. Composite extinction image of L183 (=L134N) from Pagani et al. (2004). The numbered peaks are those with molecular counterparts. Peaks 1 and 2 are candidate prestellar cold cores with dust temperatures ~ 7 K. The stripes in the right-hand panel indicate regions used to study the cloud morphology. Background stars detected in H and K' and used to estimate extinction are marked by stars and asterisks.

2005) detected a portion of the Draco nebula at a peak H I column density of $7.8 \times 10^{19} \text{ cm}^{-2}$. The cloud subtends 5 degrees on the sky and exhibits a number of compact cores and a distinct filamentary structure trailing towards high- b and high- l from the high-density complex at ($l \sim 90, b \sim 38$). Distance estimates vary with those based on Na I D absorption suggesting 463^{+192}_{-136} to 618^{+243}_{-174} pc (Gladders et al. 1998). Star count analyzes and reddening studies have resulted in significantly greater distance estimates including 800 to 2500 pc (Goerigk & Mebold 1986), and 800 to 1300 pc (Penprase et al. 2000).

CO 2.6 and 2.7 mm and H_2CO (6.2 mm) studies reveal two molecular clumps which, if the nebula is more than 800 pc distant, have masses of 27 and $219 M_{\odot}$ (Mebold et al. 1985). On the basis of virial theorem arguments these molecular clumps would be gravitationally bound for a distance to the Draco IVC exceeding 600 pc. Johnson (1986) and Johnson & Klemola (1987) examine optical counterparts to IRAS sources projected against the nebula suggesting that 33 of the optically unidentifiable sources may be similar to Bok globules although many of these may be sharp gradients in the $100 \mu\text{m}$ cirrus misidentified by the PSC source detection algorithm.

On the basis of the plume morphology seen in the IRAS $100 \mu\text{m}$ images, Odenwald & Rickard (1987) propose that the interaction of the Draco IVC with the Galactic plane is a subsonic, hydrodynamic phenomenon with a Reynolds number between ~ 10 and ~ 20 . If this interpretation is correct then we should not expect the infall of the cloud to be effective in triggering star formation along the leading edge. As the cloud is not self-gravitating, turbulent compression is needed to establish a scale hierarchy and subsequent collapse (Mac Low & Klessen 2004). Since the formation of turbulence requires Reynolds numbers greater than 100 (Odenwald & Rickard 1987), it is unlikely that the present phase of the IVC infall will result in triggered star formation. Triggered star formation will, however, become more likely in the future as the cloud moves from

the low-density, high-temperature environment of the halo into the high-density, low-temperature H I medium in the Galactic plane. There is evidence for this transition in IRAS 100 μm imaging of other cometary clouds found at $|b| > 15^\circ$ (Odenwald 1988). The clouds whose morphologies are suggestive of supersonic flow and also supporting possible star formation are preferentially at lower Galactic latitude and thus likely closer to the Galactic plane. Three of the cometary clouds studied by Odenwald (1988), G139-65, G192-67, and G225-66, are at high Galactic latitude.

MBM 55: MBM 55 ($l = 89.19, b = -40.94$) is at an estimated distance of 150 pc and is the largest high latitude translucent cloud, with a mass of $164 M_\odot$ under the assumption that ^{13}CO is in LTE (Yamamoto et al. 2003). It contains high density cores that are evident in CS(2-1) emission. This cloud is embedded along with MBM 53, HLCG 92-35, and MBM 54 in a massive $\sim 1200 M_\odot$ H I arc spanning 15 degrees on the sky (Figure 8). Yamamoto et al. (2003) find that the CO/H I ratio varies by a factor of ~ 10 across the arc indicating that the hundreds of cloudlets that comprise the arc are in different molecular stages of molecular cloud evolution. This structure is similar in morphology to the Polaris Flare (Heithausen & Thaddeus 1990).

Spectroscopic followup of RASS selected objects by Hearty et al. (1999) and Li, Hu, & Chen (2000) yielded three possible PMS stars projected near the core of MBM 55. On the basis of the weak Li I absorption exhibited by 1RXJ 2253.0+1650 and 1RXJ 2305.1+1633, the two stars in their sample that were above the main sequence, Hearty et al. (1999) concluded that both are luminosity class III or IV post-main sequence stars. As noted above, Hearty et al. (1999) interpret the majority of X-ray bright stars in this field and towards MBM 7 as part of the local ~ 150 Myr old population. Li, Hu, & Chen (2000), however, identified 1RXS J231019.1+14471 as a candidate WTTS in spite of $\text{EW}(\text{Li}) = -0.10\text{\AA}$, based on the prediction of PMS models that early M stars tend to deplete their lithium on the order of 10^6 years.

4.3. Moving Groups and Associations

Several of the pre-main-sequence stars found at $|b| > 30^\circ$ are members of local moving groups and stellar associations. The chapter on Small Loose Associations by Torres et al. in this Handbook discusses each of these groups in detail. It is worthwhile noting that high-latitude PMS stars are found in the AB Doradus moving group (HD 25457 aka HIP 18859), the kinematically similar but older Local Subgroup B4 (BD+21 418), the TW Hydrae association (HD 98800 aka TWA 4A), and the β Pictoris association (GJ 3305). These stars are within 55 pc, and thus are seen at high Galactic latitude due to their proximity to the Sun.

4.4. Isolated PMS Objects

HD 141569: Weinberger et al. (2000) identify the triple system HD 141569 as a β Pictoris-like B9.5Ve primary with comoving M2V and M4V companions separated by $1.4''$ and located at distances of $7.55''$ and $8.93''$, respectively. The estimated age based on model isochrones for the two low-mass WTTS is 5 ± 3 Myr, assuming they are at the 100 pc distance of HD 141569 determined by Hipparcos.

This system is projected near the high latitude clouds MBM 34-39 and the presence of interstellar absorption lines in the spectrum of HD 141569A; Sahu et al. (1998) conclude that it lies behind MBM 37. Weinberger et al. (2000) note that HD 141569

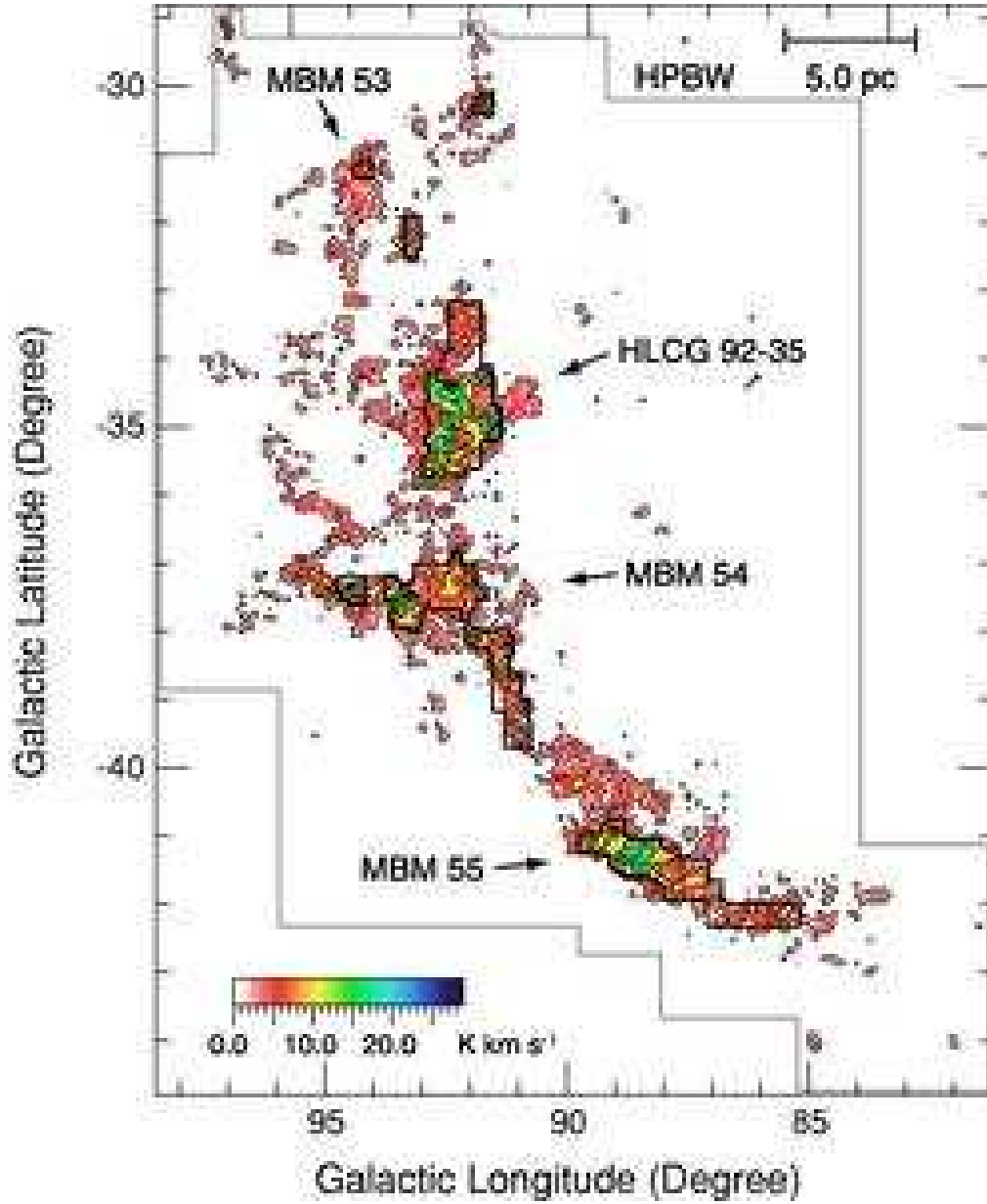


Figure 8. Total velocity-integrated intensity ^{12}CO ($J = 1-0$) map of MBM 53-55 in Galactic coordinates from Yamamoto et al. (2003). The lowest contour is 1.50 K km s^{-1} , and separation between the contours is 6.0 K km s^{-1} . The observed area of ^{12}CO is denoted by a thin solid line, and that of ^{13}CO is denoted by thick solid lines. 1RXS J231019.1+144711, the WTTS candidate identified by Li, Hu, & Chen (2000), is located just East of the main core at $(l, b) = (89.51, -41.43)$.

may not be physically associated with these clouds citing LSR radial velocity differences of $\sim 18 \text{ km s}^{-1}$ and the lack of infall signatures in the clouds. Martin-Zaïdi et al. (2005) find evidence in FUSE spectra for the diffuse outer region of L134N as well as a turbulent region of the dark cloud (as deduced from excitation of high- J levels in H_2) being present along the sightline to HD 141569A. The UVW space motion of the HD 141569 system is within two sigma of several nearby star formation associations (η Cha, TW Hya, and Tucana) suggesting a related origin.

As one of the closest Herbig AeBe stars, HD 141569A and its debris disk have been subjects of ongoing and extensive study. In their Chandra ACIS-I survey of 17 Herbig AeBe stars Stelzer et al. (2006) find that HD 141569A is one of 4 that do not exhibit X-ray emission, with $\log(L_X/L_*) < -6.8$. The low-mass companions HD 141569B and C, however, are both X-ray active having $\log(L_X/L_*) = -3.3$. HD 141569 possesses a transitional disk which Hales et al. (2006) failed to detect polarized emission from in JHK using the IRPOL2+UIST instrument at UKIRT, although the circumstellar disks around TW Hya, HD 169142, HD 150193, and HD 142666 were clearly seen. They attribute this to a relatively low peak surface brightness of $0.2 \pm 1.2 \text{ mJy arcsec}^{-2}$ for the HD 141569 disk versus $5.7 \pm 1.4 \text{ mJy arcsec}^{-2}$ for that of TW Hya.

The disk of HD 141569A exhibits a complex structure consisting of an inner clearing and two spiral rings. On the basis of dynamical simulations Ardila et al. (2005) propose that the disk is in a transient dynamical state due to a recent ($\sim 4000 \text{ yr}$) flyby of the two M dwarf companions. The event is also invoked to explain the observed dust creation rate exceeding that expected by submillimeter mass of the disk (0.33 M_\odot ; Rhee et al. 2007). Goto et al. (2006) resolved the circumstellar disk using Subaru AO+IRCS observations in CO $v=2-1$ finding that the inner clearing is $11 \pm 2 \text{ AU}$ in radius, which they interpret as close to the gravitational radius of the star, i.e. where the sound speed in the ionized medium equals the escape velocity of the system $r_g = GM_*/c_i^2$.

From an analysis of the $\text{Br}\gamma$ line profile Garcia Lopez et al. (2006) infer a mass accretion rate of $4.3 \times 10^{-9} \text{ M}_\odot/\text{yr}$. This accretion rate is surprising given the large inner hole and the apparent lack of circumstellar material (Guimarães et al. 2006). As HD 141569A is a rapid rotator ($v_* \sin i = 236 \text{ km s}^{-1}$) Brittain et al. (2007) propose that the emission may originate from a compact circumstellar disk formed by ejected material.

BP Psc: Corcoran & Ray (1997) classify Herbig Ae/Be stars into four categories based on the [O I] $\lambda 6300$ measured velocities and line profiles: I - strongly blueshifted emission, accompanied by a lower velocity blueshifted component, II - emission similar to the lower velocity component in category I, III - low velocity redshifted emission, and IV - unshifted and symmetric emission. BP Psc (aka StHA 202, PDS 103) exhibits low velocity but broad blueshifted emission placing it in category IIb, which are interpreted as Herbig Ae/Be stars having evolved past the outflow stage. BP Psc has the lowest line velocities of any star in their sample that exhibits [S II] emission.

The spectral type of BP Psc has been estimated as mid-F by Downes & Keyes (1988) and more recently as G2IVe based on spectra obtained from the HARPS echelle spectrograph at the ESO La Silla 3.6m telescope as part of the variable star one-shot project (VSOP) (Dall et al. 2007). Suárez et al. (2006) also assign a spectral type of G2e to BP Psc as part of their follow-up observations of objects having IRAS FIR colors similar to planetary nebulae.

However, due to an extensive multiwavelength observation program by Zuckerman et al. (2008) the PMS status of BP Psc is now in doubt. In spite of the presence of emission line bi-polar jets and evidence for gas accretion, Zuckerman et al. (2008) suggest that BP Psc may be a first-ascent, post-main sequence giant star whose accretion and out-flows are due to a low-mass companion possibly consumed during a recent common envelope phase.

The list BP Psc's intriguing features include $^{12}\text{CO}(2-1)$ and $^{12}\text{CO}(3-2)$ emission, which are rare in isolated high Galactic latitude main sequence and PMS stars and unknown in first-ascent giant stars, an extremely compact circumstellar disk ($< 0.2''$), and a very large fraction ($\sim 75\%$) of the stellar bolometric luminosity being reprocessed by grains. The optical and near-IR spectral features include those consistent with a PMS nature such as a broad ($\text{EW} = -11$ to -15 \AA) $\text{H}\alpha$ emission line, numerous forbidden emission lines, and a v_{tini} of $32.3 \pm 1.2 \text{ km s}^{-1}$ suggestive of youth. However, the EW of the lithium 6709.6 \AA line is only 50 m\AA , which is more appropriate for K-type stars older than 100 Myr. In addition, analysis of surface gravity sensitive features indicate $\log(g) \sim 2.5$, an order of magnitude weaker than that expected for a PMS star.

Zuckerman et al. (2008) conclude that uncovering the true nature of BP Psc will require a direct measurement of its trigonometric parallax in order to determine its luminosity. If BP Psc is a PMS star, then the challenges of the apparent low surface gravity and lack of photospheric lithium must be dealt with. In the alternative scenario BP Psc may be the first example of a rare stage in the post-main sequence evolution of close binary systems.

GSC 04744-01367: Both members of this $6''$ wide binary, cataloged as PDS 11a/b by Gregorio-Hetem et al. (1992), exhibit $\text{H}\alpha$ emission, although Li absorption is only seen in the northern (a) component. No spectral type is specified although the photometry given by Gregorio-Hetem et al. (1992) ($B - V = 1.51, 1.34$ and $V - I = 2.21, 2.24$) for the two components are consistent with an early M spectral type (Reid & Hawley 2000). The minimum photometric distances computed using the main sequence ($M_V, V - I$) relation in Reid & Hawley (2000) and based on the $V - I$ colors and V magnitudes of $V = 14.76, 15.34$ are 77 and 97 pc, respectively.

TYC 8474-24-1: TYC 8474-24-1, aka PDS 2 (Gregorio-Hetem et al. 1992), is an isolated Herbig Ae/Be star of spectral type F3V (Vieira et al. 2003). The photometric distance as a main sequence star is 340 pc, so at $b = -64.1^\circ$ the star's minimum height below the Galactic plane is 306 pc.

5. Discussion: Environment and Processes of High-latitude Star Formation

There are three distinct populations of pre-main-sequence stars seen at high Galactic latitudes. These are those still found in association with their parent molecular clouds, those found in isolation far from any present molecular cloud, and those formed in extraplanar environments high above the Galactic plane.

The processes that result in isolated T Tauri stars include ejection of the young star and dissipation of the parent cloud. If dynamical ejection velocities are as high as $\sim 5 \text{ km/sec}$, over the typical 10 Myr lifetime of the Classical T Tauri phase a star may have traveled 50 pc resulting in separations from their birthplace by 10's of degrees on the sky (for distances of a few 100 pc).

The known high-latitude star formation sites include both gravitationally bound (MBM 20) and unbound (MBM 12) clouds. When star formation occurs within an unbound cloud the cloud dissipates on timescales of a few Myr, even without massive O/B stars present. It is possible that outflows from low-mass stars may drive the dissipation (Sterzik & Durisen 1995; Feigelson 1996; Hartmann, Ballesteros-Paredes, & Bergin 2001).

5.1. Determining Association between PMS Stars and Clouds

The example of HD 141569 illustrates the difficulty of associating PMS candidates with high-latitude clouds. There are three major issues determining the association between a PMS star and a cloud. The first is that candidate PMS stars are seldom projected against the cores of the clouds. This is in contrast to IRAS studies of PMS stars associated with dark cloud cores, e.g. Wood et al. (1994), and forces us to make proximity arguments. The second issue is that the spatial velocity of the candidate PMS star can be very discrepant with that of the gas. Models of T Tauri migration predict velocity dispersions of $\sim 1 \text{ km s}^{-1}$ inherited from thermal motions in the parent cloud (Feigelson 1996). While dynamic ejection can, as stated above, result in velocity dispersions an order of magnitude greater, this process may be less effective in the lower density environments of the high latitude star formation regions.

The third complication is that the distances to both the cloud and to the PMS star are usually poorly determined. Cloud distances can be inferred by techniques such as comparison of off-cloud and on-cloud star counts, bracketing of cloud location by the detection of reddening in stellar colors and absorption features in the spectra of early type stars, and by statistical estimates based on an assumed dust scale height above the Galactic plane.

The luminosity of a PMS star as it descends down its nearly isothermal Hayashi track has a steep dependency on the stellar age and mass (Baraffe et al. 1998). In order to accurately determine the intrinsic luminosity of a PMS star, and thus its distance, the photometry and spectra must be analyzed and compared against evolutionary models.

5.2. High-latitude Stellar Nurseries

The low density environment found in high-latitude clouds creates a challenge for low-mass star formation via direct gravitational collapse. One scenario is that stars are created at the low density limit of the normal formation process, i.e. gravitational collapse of low mass cores. There are a handful of star formation regions found in high-latitude molecular clouds, e.g. in MBM 12 and MBM 20.

Both MBM 12 and MBM 20 are Lynds dark clouds thus the column density of H_2 in their densest regions is higher by an order of magnitude than for typical translucent high-latitude clouds. We suspect these are the closest star formation regions to the Sun - besides Na D studies, color excess, etc., in a statistical sense we know these predominately translucent clouds are nearby because they are more numerous in the southern Galactic hemisphere (the Sun is ~ 14 pc north of the midplane).

Until recently MBM 12 was considered the nearest star-forming region, however recent work (Luhman 2001; Andersson et al. 2002) has placed it at ~ 275 pc, so that it is significantly farther out than the Taurus or Ophiuchus star forming regions. MBM 20 may now be the closest star forming region, but its distance is not well-constrained, with estimates ranging from 100 to 160 pc.

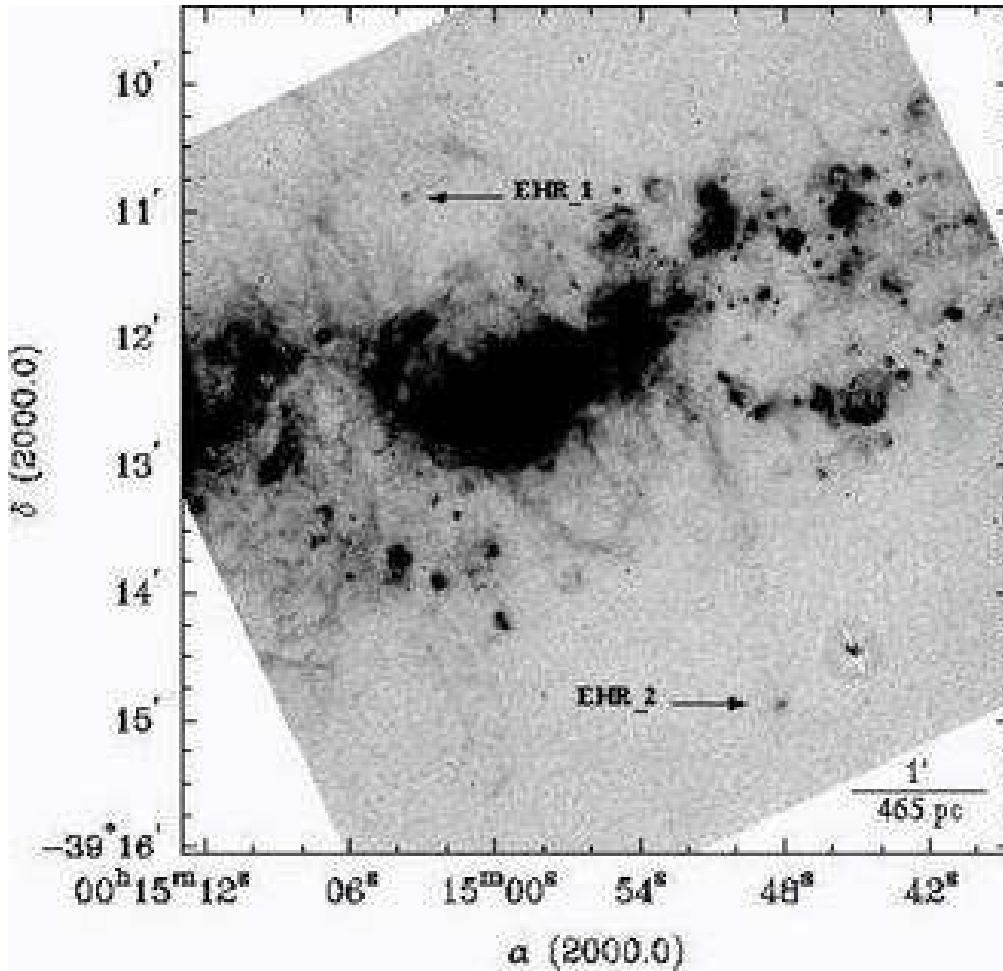


Figure 9. This $H\alpha$ image from the VLR FORS instrument of the nearby edge-on spiral galaxy NGC 55 (Tuellmann et al. 2003) shows two extraplanar H II regions. Hydrodynamic considerations suggest that the high-mass star formation occurred in-situ.

5.3. Isolated High-latitude PMS Stars

High-latitude PMS stars found in isolation may be the result of either ejection from or dissipation of the parent cloud. Dissipation timescales for unbound clouds appear to be a few Myr. The formation scenarios for low-mass isolated T Tauri stars include normal modes of formation within a molecular cloud followed by dissipation of the parent cloud and/or dynamical ejection of the young star. The population of dispersed Weak-lined T Tauri stars (WTTS) is doubtless underestimated since due to the absence of magnetospheric accretion and disk signatures they are nearly indistinguishable from the numerous active M dwarfs (dMe) in the field.

5.4. Extraplanar Star Formation Regions

In the Second and Third Galactic quadrants we are afforded a view of the disk-halo interface relatively free of interstellar extinction and obscuration by the Galactic bulge population. This provides the opportunity of an optical survey of stellar populations formed in-situ in the Galactic halo. In nearby edge-on spirals, for example NGC 55 in the Sculptor group, there is clear evidence for OB associations found high above the Galactic disk (Tuellmann et al. 2003, see Figure 9). Hydrodynamic considerations suggest that the high-mass star formation occurred in-situ. The signatures of Galactic high-latitude massive star formation include H II regions (Sharpless 1959; Gillespie et al. 1977; Blitz, Fich, & Stark 1982) that would be detected via imaging and H α surveys, e.g. Reynolds et al. (2005).

The interpretation of these objects, however, can be problematic as shown by examination of the presumed H II regions cataloged by Sharpless (1959). Out of the 8 high-latitude Sharpless regions, 2 are planetary nebulae and the remainder are dust reflection nebulae or photoluminescence of C in molecular clouds, thus none are bona fide H II regions. The specific identifications for the planetary nebulae are PN A55 20 and PN A55 24 (Abell 1955) for Sh2-290 and Sh2-313. Sh2-24, Sh2-33, Sh2-36, Sh2-73, Sh2-122, and Sh2-245, which are the other Sharpless regions at $|b| \geq 30^\circ$, are associated with the molecular clouds MBM 57, MBM 38, MBM 38, MBM 40, MBM 55, and MBM 18, respectively (Blitz, Fich, & Stark 1982; Magnani, Blitz, & Mundy 1985).

Nyman et al. (1987) find a large molecular cloud in Lupus that is far from the Galactic plane. At an assumed distance of 2.9 kpc, this cloud is 150 to 280 pc above the plane. The relative lack of CO emission in the plane below the cloud, with a diameter of ~ 200 pc, suggest that stellar winds and/or supernovae may have formed both structures. Nyman et al. (1987) point out a semblance to the local Gould Belt and a relation, albeit on different scales, to H I shells and Galactic fountains.

A possible formation scenario involves a star formation episode within the disk ejecting gas into the halo. This gas subsequently cooled down forming H I and possibly molecular clouds. Winds and shocks from later disk star formation episodes then trigger star formation in these clouds (Elmegreen 1998). Presumably low-mass star formation would be triggered as well although these would not be detected in H α surveys of external galaxies such as Tuellmann et al. (2003). This association of triggered star formation within the halo with shocked gas from superbubbles and Galactic fountain events is relevant to the search for stellar populations in Intermediate and High Velocity Clouds (IVCs and HVCs). Moreover, if stellar populations are indeed formed within the halo from disk gas transported out of the plane by massive star winds and supernovae, they should combine near-solar metallicities with non-disk kinematics due to ejection and infall.

Deep and high-resolution optical imaging of massive (L_*) edge-on spiral galaxies reveals that extraplanar ($|z| > 0.4$ kpc) dust structures are found in association with extraplanar H α emission (Howk & Savage 1999; Thompson et al. 2004). Both the dust and the H α emission are seen above most of the thin disk molecular material. The largest structures have gas masses $> 10^5 M_\odot$ with implied potential energies $> 10^{52}$ erg. The morphologies of some of the extraplanar dust structures suggest production via supernova-driven galactic fountain or chimney phenomena. Other extraplanar features, for example as seen in NGC 4217, are not readily linked to high-energy events in the disk.

6. Summary

The high latitude population of molecular clouds is mostly translucent. Although molecular cores have been identified in translucent clouds and even in Galactic cirrus, the only verified stellar nurseries are MBM 12 and MBM 20, which are both dark clouds. Thus, at the very least, the star formation rate in translucent clouds is significantly less than in dark clouds. Is this a consequence of column density, which is the most obvious distinction between dark and translucent clouds, rather than density within the cloud?

The ability of at least a few high latitude clouds to form cold molecular cores and young stars may be due to a combination of conditions including variations in the interstellar radiation field, changes in dust grain size and chemistry, and the occurrence of shocks and other transient events in the ISM. Regardless of the formation mechanisms, study of the high latitude star formation environment continues to be an intriguing field.

Acknowledgments. I am thankful to Loris Magnani for a detailed and helpful referee's report. This research has made extensive use of the SIMBAD database, operated at CDS, Strasbourg, France, and NASA's Astrophysics Data System.

References

- Abell, G. O. 1955, *PASP*, 67, 258
- Akyilmaz, M., Flower, D. R., Hily-Blant, P., Pineau Des Forêts, G., & Walmsley, C. M. 2007, *A&A*, 462, 221
- Andersson, B.-G., Idzi, R., Uomoto, A. et al. 2002, *AJ*, 124, 2164
- Appenzeller, I., Thiering, I., Zickgraf, F.-J. et al. 1998, *ApJS*, 117, 319
- Ardila, D. R., Lubow, S. H., Golimowski, D. A. et al. 2005, *ApJ*, 627, 986
- Baraffe, I., Chabrier, G., Allard, F., & Hauschildt, P. H. 1998, *A&A*, 337, 403
- Beichman, C. A., Myers, P. C., Harris-Law, S., Mathieu, R., Benson, P. J., & Jennings, R. E. 1986, *ApJ*, 307, 337
- Blaauw, A. 1991, *The Physics of Star Formation and Early Stellar Evolution*, C. J. Lada & N. D. Kylafis (eds.), Kluwer Acad. Press, p. 125
- Blitz, L., Fich, M., & Stark, A. A. 1982, *ApJS*, 49, 183
- Bohlin, R. C., Savage, B. D., & Drake, J. F. 1978, *ApJ*, 224, 132
- Brittain, S. D., Simon, T., Najita, J. R., & Rettig, T. W. 2007, *ApJ*, 659, 685
- Broeg, C., Joergens, V., Fernández, M., Husar, D., Hearty, T., Ammler, M., & Neuhäuser, R. 2006, *A&A*, 450, 1135
- Caillault, J.-P., Magnani, L., & Fryer, C. 1995, *ApJ*, 441, 261
- Carpenter, J. M., Wolf, S., Schreyer, K., Launhardt, R., & Henning, T. 2005, *AJ*, 129, 1049
- Chaplin, V. H., Larson, K. A., & Gerakines, P. A. 2004, *Bulletin of the American Astronomical Society*, 36, 1439
- Chastain, R. J., Shelton, R. L., Raley, E. A., & Magnani, L. 2006, *ApJ*, 132, 1964
- Chauvin, G., Ménard, F., Fusco, T., Lagrange, A.-M., Beuzit, J.-L., Mouillet, D., & Augereau, J.-C. 2002, *A&A*, 394, 949
- Comeron F. & Torra J. 1992, *A&A*, 261, 94
- Comeron F. & Torra J. 1994, *A&A*, 281, 35
- Corcoran, M. & Ray, T. P. 1997, *A&A*, 321, 189
- Cox, D. P. & Reynolds, R. J. 1987, *ARA&A*, 25, 303
- Dall, T. H., Foellmi, C., Pritchard, J. et al. 2007, *A&A*, 470, 1201
- Danziger, J. I. & Gilmozzi, R. 1997, *A&A*, 323, 47
- Davis, C. J., Ray, T. P., Eisloffel, J., & Corcoran, D. 1997, *A&A*, 324, 263
- Davis, C. J., Matthews, H. E., Ray, T. P., Dent, W. R. F., & Richer, J. S. 1999, *MNRAS*, 309, 141

- Désert, F. X., Bazell, D., & Boulanger, F. 1988, ApJ, 334, 815
- de Vries, H. W., Heithausen, A., & Thaddeus, P. 1987, ApJ, 319, 723
- Downes, R. A. & Keyes, C. D. 1988, AJ, 96, 777
- Dutra, C. M. & Bica, E. 2002, A&A, 383, 631
- Elmegreen, B. G. 1998, in ASP Conf. Series No. 148 *Origins*, eds. C.E. Woodward et al., 150
- Emprechtinger, M., Kimeswenger, S., Kronberger, T. et al. 2005, AN, 326, 115
- Evans, N. J., II & Kutner, M. L. 1976, ApJ, 204, L131
- Feigelson, E. D., Jackson, J. M., Mathieu, R. D., Myers, P. C., & Walter, F. M. 1987, AJ, 94, 1251
- Feigelson, E. D. 1996, ApJ, 468, 306
- Feigelson, E. D. & Decampli, W. M. 1981, ApJ, 243, L89
- Feigelson, E. D., Lawson, W. A., Stark, M., Townsley, L., & Garmire, G. P. 2006, AJ, 131, 1730
- Franco, G. A. P. 1989, A&A, 223, 313
- Fuhrmeister, B. & Schmitt, J. H. M. M. 2003, A&A, 403, 247
- Garcia Lopez, R., Natta, A., Testi, L., & Habart, E. 2006, A&A, 459, 837
- Giacconi, R., Branduardi, G., Briel, U. et al. 1979, ApJ, 230, 540
- Gillespie, A. R., Huggins, P. J., Sollner, T. C. L. G. et al. 1977, A&A, 60, 221
- Gladders, M. D., Clarke, T. E., Burns, C. R. et al. 1998, ApJ, 507, L161
- Goerigk, W., Mebold, U., Reif, K., Kalberla, P. M. W., & Velden, L. 1983, A&A, 120, 63
- Goerigk, W. & Mebold, U. 1986, A&A, 162, 279
- Goto, M., Usuda, T., Dullemond, C. P., Henning, T., Linz, H., Stecklum, B., & Suto, H. 2006, ApJ, 652, 758
- Gould B. A., 1879, *Uranometria Argentina*, ed. P.E. Corni, Buenos Aires, p. 354
- Gregorio-Hetem, J., Lepine, J. R. D., Quast, G. R., Torres, C. A. O. & de La Reza, R. 1992, AJ, 102, 549
- Gregorio-Hetem, J., Castilho, B. V., & Barbuy, B. 1993, A&A, 268, L25
- Guhathakurta, P. & Tyson, J. A. 1989, ApJ, 346, 773
- Guillout, P., Sterzik, M. F., Schmitt, J. H. M. M., Motch, C., & Neuhauser, R. 1998, A&A, 337, 113
- Guimarães, M. M., Alencar, S. H. P., Corradi, W. J. B., & Vieira, S. L. A. 2006, A&A, 457, 581
- Gyul' Budagyan, A. L. 1982, Pis'ma v Astronomicheskii Zhurnal, 8, 232
- Gyul' Budagyan, A. L., Glushkov, Yu. I., & Denisyuk, E. K. 1978, ApJ, 224, L137
- Hales, A. S., Gledhill, T. M., Barlow, M. J., & Lowe, K. T. E. 2006, MNRAS, 365, 1348
- Hartmann, D., Magnani, L., & Thaddeus, P. 1998, ApJ, 492, 205
- Hartmann, L., Ballesteros-Paredes, J., & Bergin, E. A. 2001, ApJ, 562, 852
- Hartmann, D. & Burton, W. B. 1997, *Atlas of Galactic Neutral Hydrogen* (NY: Cambridge University Press)
- Hearty, T., Magnani, L., Caillault, J.-P. et al. 1999, A&A, 341, 163
- Hearty, T., Neuhauser, R., Stelzer, B. et al. 2000, A&A, 353, 1044
- Hearty, T., Fernández, M., Alcalá, J. M. et al. 2000, A&A, 357, 681
- Heiles, C. & Habing, H. J. 1974, A&AS, 14, 1
- Heiles, C., Reach, W. T., & Koo, B.-C. 1988, ApJ, 332, 313
- Heithausen, A., Bertoldi, F., & Bensch, F. 2002, A&A, 383, 591
- Heithausen, A. & Thaddeus, P. 1990, ApJ, 353, L49
- Herbig, G. H. & Bell, K. R. 1988, Lick Observatory Bulletin No. 1111
- Herbig, G. H., Vrba, F. J., & Rydgren, A. E. 1986, AJ, 91, 575
- Hobbs, L. M., Penprase, B. E., Welty, D. E., Blitz, L., & Magnani, L. 1988, ApJ, 327, 356
- Hogerheijde, M. R., Jayawardhana, R., Johnstone, D. et al. 2002, AJ, 124, 3387
- Hogerheijde, M. R., Johnstone, D., Matsuyama, I., Jayawardhana, R., & Muzerolle, J. 2003, ApJ, 593, L101
- Honda, M., Kataza, H., Okamoto, Y. K. et al. 2006, ApJ, 646, 1024
- Howk, J. C. & Savage, B. D. 1999, AJ, 117, 2077
- Humason, M. L. & Zwicky, F. 1947, ApJ, 105, 85
- Itoh, Y., Sugitani, K., Fukuda, N. et al. 2003, ApJ, 586, L141
- Johnson, H. M. 1986, ApJ, 309, 321

- Johnson, H. M. & Klemola, A. R. 1987, *ApJS*, 63, 701
- Joint Science Working Group 1985, *IRAS Point Source Catalog* (Washington, D.C.: US GPO)
- Keto, E. R. & Myers, P. C. 1986, *ApJ*, 304, 466
- Kirk, J. M., Ward-Thompson, D., & André, P. 2005, *MNRAS*, 360, 1506
- Kun, M. 1992, *A&A Suppl.* 92, 875
- Kuntz, K. D., Snowden, S. L., & Verter, F. 1997, *ApJ*, 484, 245
- Larson, K. A. & Reed, C. M. 2003, in *Astrophysics of Dust*, ed. A.N. Witt
- Lehtinen, K., Juvela, M., Mattila, K., Lemke, D., & Russeil, D. 2007, *A&A*, 466, 969
- Li, J. Z. & Hu, J.-Y. 1998, *ApJS*, 132, 173
- Li, J. Z., Hu, J.-Y., & Chen, W. P. 2000, *A&A*, 356, 157
- Li, J. Z. 2004, *Chinese J. Astron. Astrophys.*, 4, 2004
- Liljeström, T., Mattila, K., & Friberg, P. 1989, *A&A*, 210, 337
- Lockman, F. J. & Condon, J. J. 2005, *AJ*, 129, 1968
- López-Santiago, J., Montes, D., Crespo-Chacón, I., & Fernández-Figueroa, M. J. 2006, *ApJ*, 643, 1160
- Luhman, K. L. 2001, *ApJ*, 560, 287
- Luhman, K. L. & Steeghs, D. 2004, *ApJ*, 609, 917
- Lynds, B. T. 1962, *ApJS*, 12, 163
- Lynds, B. T. 1965, *PASP*, 77, 134
- Lynds, B. T. 1965, *ApJS*, 12, 163
- Mac Low, M. -M. & Klessen, R. S. 2004, *Rev. Mod. Phys.* 78, 125
- Maheswar, G., Manoj, P., & Bhatt, H. C. 2004, *A&A*, 402, 963
- Magazzu, A., Martin, E. L., Sterzik, M. F., Neuhauser, R., Covino, E., & Alcalá, J. M. 1997, *A&AS*, 124, 449
- Magnani, L., Blitz, L., & Mundy, L. 1985, *ApJ*, 295, 402 (MBM)
- Magnani, L., Caillaut, J.-P., & Armus, L. 1990, *ApJ*, 357, 602
- Magnani, L., Caillaut, J.-P., Buchalter, A. & Beichman, C. A. 1995, *ApJS*, 96, 159
- Magnani, L., Chastain, R. J., Kim, H. C., Hartmann, D., Truong, A. T., & Thaddeus, P. 2003, *ApJ*, 586, 1111
- Magnani, L., Hartmann, D., & Speck, B. G. 1996, *ApJS*, 106, 447
- Magnani, L., Hartmann, D., Holcomb, S. L., Smith, L. E., & Thaddeus, P. 2000, *ApJ*, 535, 167
- Martin, E. L. & Kun, M. 1996, *A&A Suppl.*, 116, 467
- Martin, E. L. & Magazzú, A. 1999, *A&A*, 342, 173
- Martin, J. C. 2004, *AJ*, 128, 2474
- Martin, J. C. 2006, *AJ*, 131, 3047
- Martin-Zaïdi, C., Deleuil, M., Simon, T., Bouret, J.-C., Roberge, A., Feldman, P. D., Lecavelier Des Etangs, A., & Vidal-Madjar, A. 2005, *A&A*, 440, 921
- McLaughlin, D. E. & Pudritz, R. E. 1997, *ApJ*, 476, 750
- Mebold, U., Cernicharo, J., Velden, L., Reif, K., Crezelius, C., & Goerigk, W. 1985, *A&A*, 151, 427
- Mercer, E. P., Clemens, D. P., Bania, T. M. et al. 2004, *ApJS*, 154, 328
- Meyerdierks, H., Heithausen, A., & Reif, K. 1991, *A&A*, 245, 247
- Moriarty-Schieven, G. H., Andersson, B.-G., & Wannier, P. G. 1997, *ApJ*, 475, 642
- Moshir, M., Copan, G., Conrow, T. et al. 1989, *IRAS Faint Source Catalog Explanatory Supplement*
- Myers, P. C., Fuller, G. A., Mathieu, R. D., Beichman, C. A., Benson, P. J., Schild, R. E., & Emerson, J. P. 1987, *ApJ*, 319, 340
- Neuhauser, R., Sterzik, M. F., Torres, G., & Martin, E. L. 1995, *A&A*, 299, L13
- Neuhauser, R., Torres, G., Sterzik, M., & Randich, S. 1997, *A&A*, 325, 647
- Nyman, L.-A., Thaddeus, P., Bronfman, L., & Cohen, R. S. 1987, *ApJ*, 314, 374
- Odenwald, S. F. & Rickard, L. J. 1987, *ApJ*, 318, 702
- Odenwald, S. F. 1988, *ApJ*, 325, 320
- Otero, S. A., Wils, P., & Dubovsky, P. A. 2005, *Informational Bulletin on Variable Stars*, No. 5586,
- Pagani, L., Bacmann, A., Motte, F. et al. 2004, *A&A*, 417, 605

- Pagani, L., Bacmann, A., Cabrit, S., & Vastel, C. 2007, A&A, 467, 179
- Penprase, B. E., Rhodes, J. D., & Harris, E. L. 2000, A&A, 364, 712
- Pinzón, G., Seifahrt, A., & de La Reza, R. 2006, Revista Mexicana de Astronomía y Astrofísica Conference Series, 26, 41
- Pound, M. W. & Blitz, L. 1993, ApJ, 418, 328
- Reach, W. T., Wall, W. F., & Odegard, N. 1998, ApJ, 507, 507
- Reid, N. & Hawley, S. L. 2000, *New light on dark stars : red dwarfs, low mass stars, brown dwarfs* New York : Springer, (Springer-Praxis series in astronomy and astrophysics)
- Reipurth, B. & Heathcote, S. 1990, A&A, 229, 527
- Reipurth, B. & Zinnecker, H. 1993, A&A, 278, 81
- Requena-Torres, M. A., Marcelino, N., Jiménez-Serra, I., Martín-Pintado, J., Martín, S., & Mauersberger, R. 2007, ApJ, 655, L37
- Reynolds, R. J., Chaudhary, V., Madsen, G. J. et al. 2005, AJ, 129, 927
- Rhee, J. H., Song, I., Zuckerman, B., & McElwain, M. 2007, ApJ, 660, 1556
- Ridderstad, M., Juvela, M., Lehtinen, K., Lemke, D., & Liljeström, T. 2006, A&A, 451, 961
- Sahu, M. S., Blades, J. C., He, L., Hartmann, D., Barlow, M. J., & Crawford, I. A. 1998, ApJ, 504, 522
- Sandage, A. 1976, AJ, 81, 954
- Sandell, G., Reipurth, B., & Gahm, G. 1987, A&A, 171, 283
- Schachter, J. F., Remillard, R., Saar, S. H., Favata, F., Sciortino, S., & Barbera, M. 1996, ApJ, 463, 747
- Schlegel, D. J., Finkbeiner, D. P., & Davis, M. 1998, ApJ, 500, 525
- Sharpless, S. 1959, ApJS, 4, 257
- Silverstone, M. D., Meyer, M. R., Mamajek, E. E. et al. 2006, ApJ, 639, 1138
- Smith, G. H. & Shetrone, M. D. 2000, PASP, 112, 1320
- Stark, A. A. & Lee, Y. 2005, ApJ, 619, L159
- Stephenson, C. B. 1986, ApJ, 300, 779
- Stelzer, B., Micela, G., Hamaguchi, K., & Schmitt, J. H. M. M. 2006, A&A, 457, 223
- Sterzik, M. F. & Durisen, R. H. 1995, A&A, 304, 9
- Straizys, V., Černis, K., Kazlauskas, A., & Laugalys, V. 2002, Baltic Astronomy, 11, 231
- Suárez, A., Garcia-Lario, P., Manchado, A. et al. 2006, A&A, 458, 173
- Thompson, T. W. J., Howk, J. C., & Savage, B. D. 2004, AJ, 128, 662
- Torres, C. A. O., Quast, G., de la Reza, R., Gregorio-Hetem, J., & Lepine, J. R. D., 1995, AJ, 109, 2146
- Torres, C. A. O., da Silva, L., Quast, G. R., de la Reza, R., & Jilinski, E. 2000, AJ, 120, 1410
- Torres, C. A. O., Quast, G. R., da Silva, L., de La Reza, R., Melo, C. H. F., & Sterzik, M. 2006, A&A, 460, 695
- Trümpler, J. 1983, Adv. Space. Res., 2, 241
- Tuellmann, R., Rosa, M. R., Elwert, T. et al. 2003, *The Messenger* (European Southern Observatory), 114, 39
- van Dishoeck, E. F. & Black, J. H. 1988, ApJ, 334, 771
- van Dishoeck, E. F. & Black, J. H. 1989, ApJ, 340, 273
- Vieira, S. L. A., Corradi, W. J. B., Alencar, S. H. P., Mendes, L. T. S., Torres, C. A. O., Quast, G. R., Guimarães, M. M., & da Silva, L. 2003, AJ, 126, 2971
- Wakker, B. P. 2001, ApJS, 136, 463
- Weaver, W. B. & Hobson, S. W. 1988, PASP, 100, 1443
- Weinberger, A. J., Rich, R. M., Becklin, E. E., Zuckerman, B., & Matthews, K. 2000, ApJ, 544, 937
- Wichmann, R., Sterzik, M., Krautter, J., Metanowski, A., & Voges, W. 1997, A&A, 326, 211
- Williams, E. G. 1934, ApJ, 79, 280
- Wood, D. O. S., Myers, P. C., & Daugherty, D. A. 1994, ASP Conf. Ser. 65, *Clouds, Cores, and Low Mass Stars*, ed. D.P. Clemens & R. Barvainis, 14
- Xing, L.-F., Shi, J.-R., & Wei, J.-Y. 2007, New Astronomy, 12, 265
- Xing, L. F., Zhang, X. B., & Wei, J. Y. 2007, New Astronomy, 12, 346
- Yamamoto, H., Onishi, T., Mizuno, A., & Fukui, Y. 2003, ApJ, 592, 217

- Zuckerman, B., Song, I., Bessell, M. S., & Webb, R. A. 2001, *ApJ*, 562, L87
Zuckerman, B. & Song, I. 2004, *ARA&A*, 42, 685
Zuckerman, B., Song, I., & Bessell, M. S.. 2004, *ApJ*, 613, L65
Zuckerman, B., Melis, C., Song, I. et al. 2008, arXiv:0802.0226v2 [astro-ph]